

STAR Time-Projection Chamber

Huan Zhong Huang

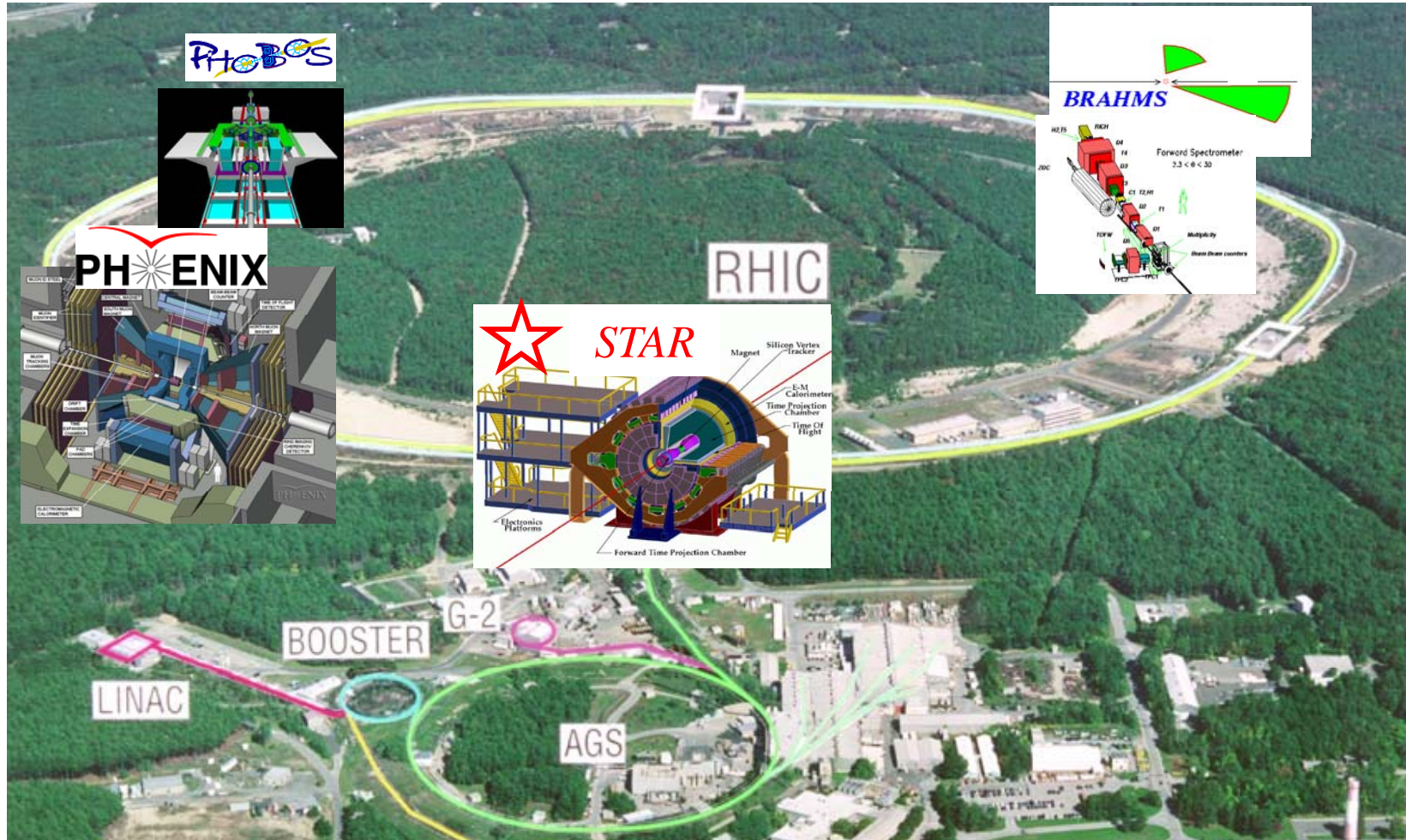
**Department of Engineering Physics
Tsinghua University**

&

**Department of Physics and Astronomy
University of California, Los Angeles**

**Thanks to Gene Van Buren, Jim Thomas,
Blair Stringfellow and Howard Wieman**

Relativistic Heavy Ion Collider --- RHIC



Au+Au 200 GeV N-N CM energy
Polarized p+p up to 500 GeV CM energy

STAR Physics Approaches

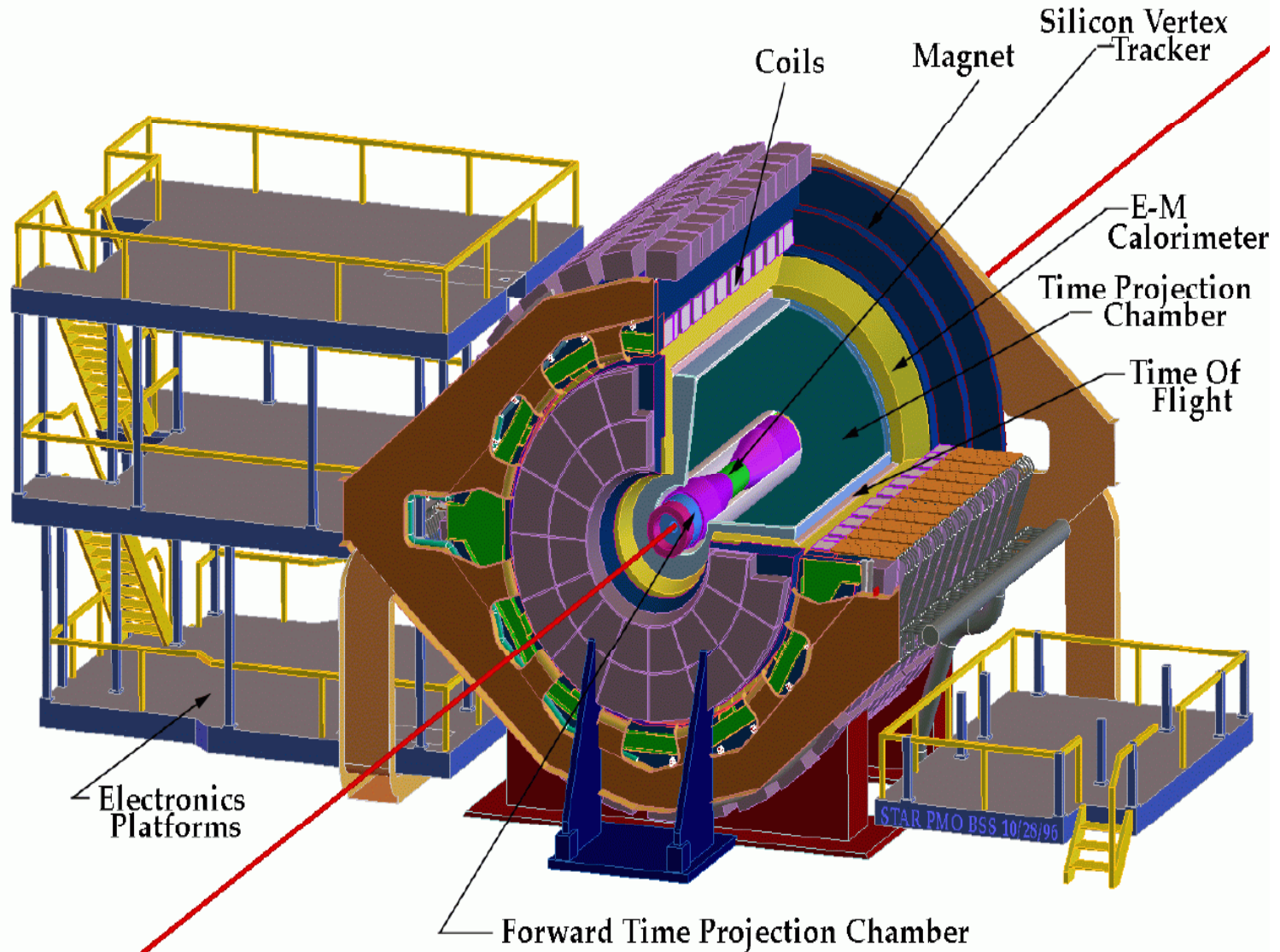
Emphasis on Observables Sensitive to Early Partonic Stages:

- 1) High p_T particles – Jet quenching? New baryon dynamics?
- 2) Particle fluctuations and large scale correlations – probe conditions near phase boundary.
- 3) Partonic collective flow observables especially for those particles believed to have small hadronic re-scattering cross sections ϕ , Ω , D mesons and J/ψ .
- 4) D meson production for initial gluon flux and structure function of nuclei.
- 5) J/ψ for possible color screening effect
- 6) Direct and thermal photon production

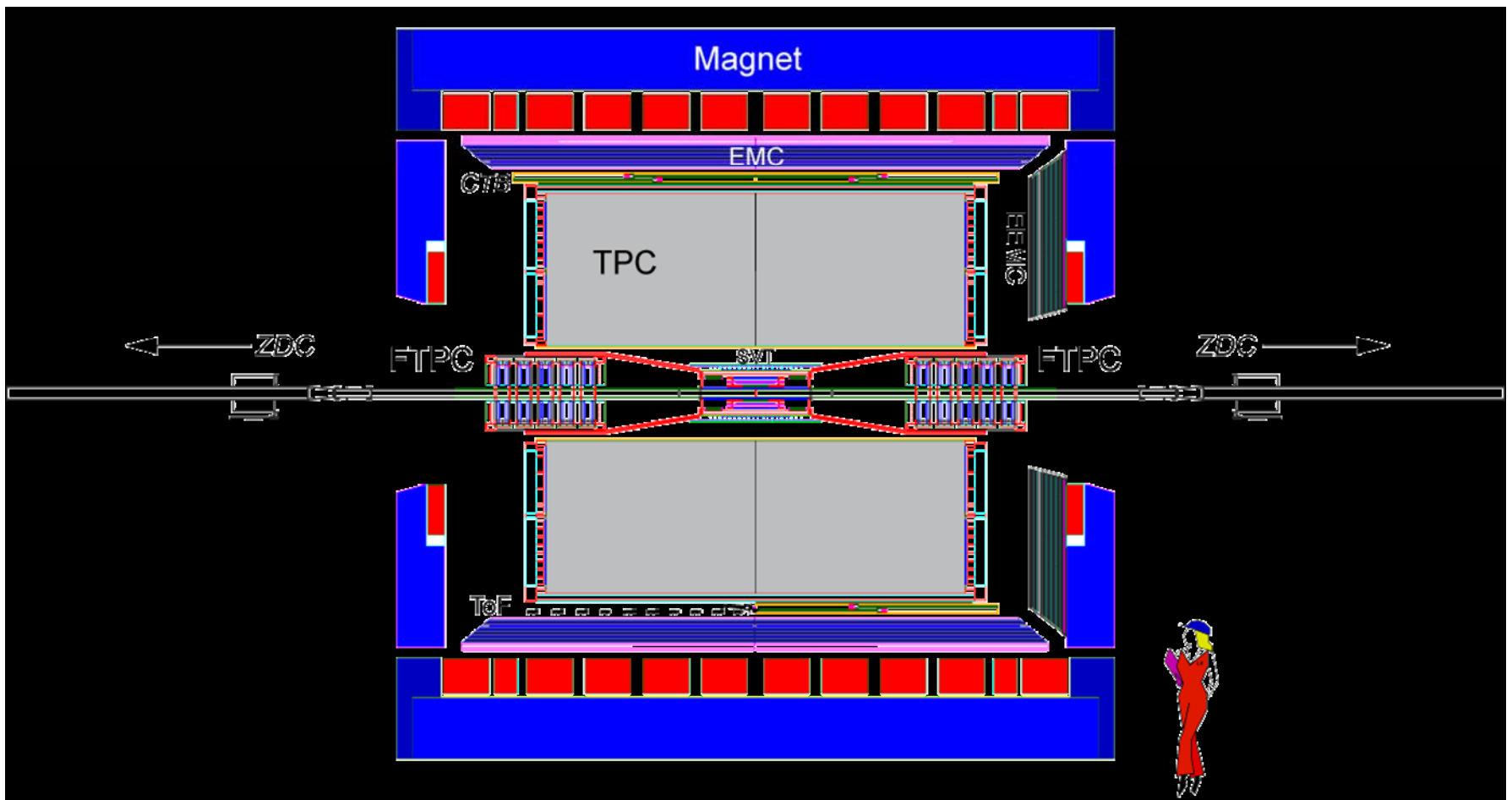
Precision Measurements to Map Out Hadronic Evolution Dynamics

- 1) Resonances (ρ , Δ , f_0 , K^* , ϕ , $\Sigma(1385)$ and $\Lambda(1520)$) – Sensitive to hadronic evolution between chemical and kinetic freeze-out
- 2) Momentum-space-time relations at the kinetic freeze-out thru correlations of identical, non-identical pairs, and light clusters.

STAR Schematic

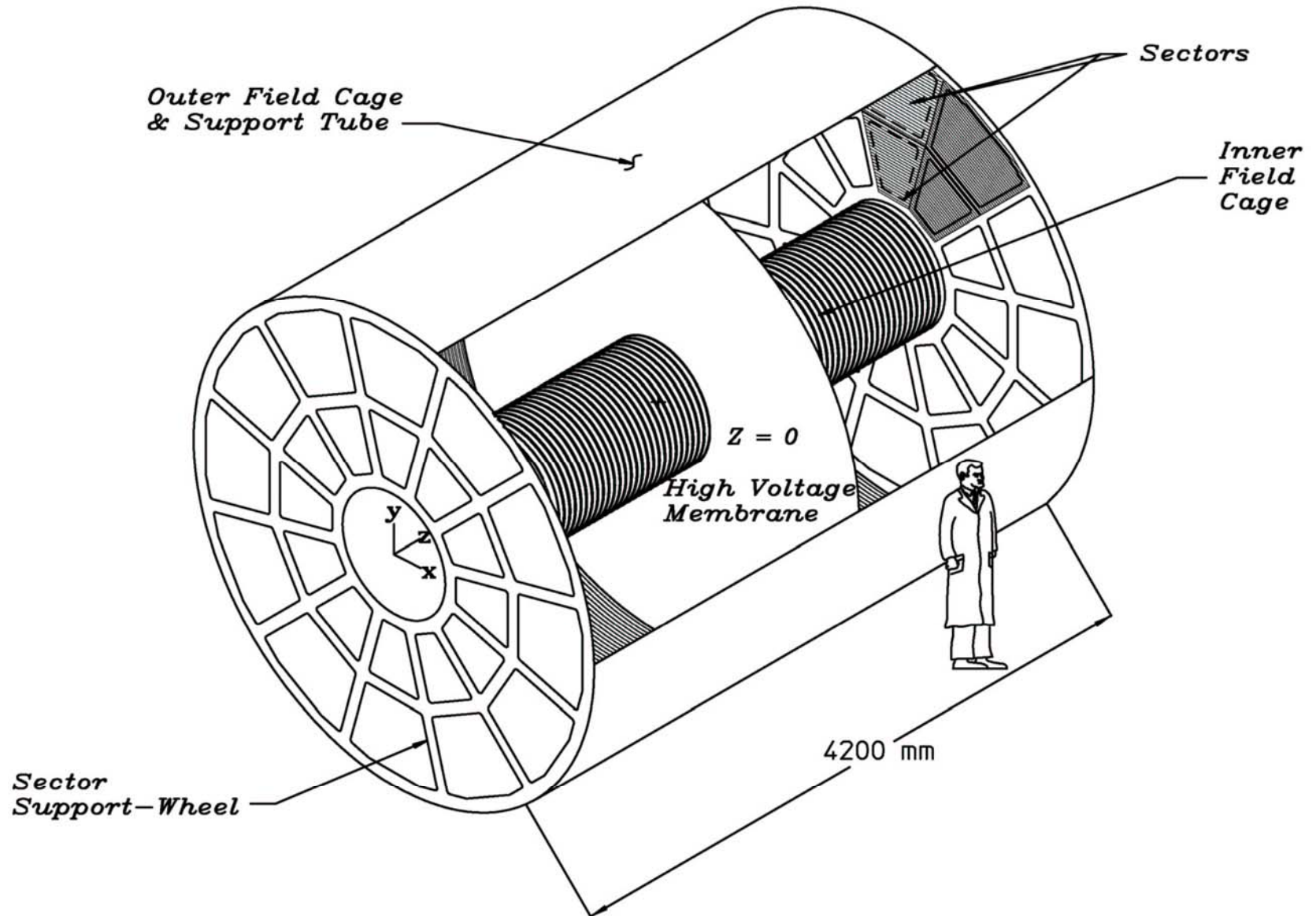


The STAR Detector

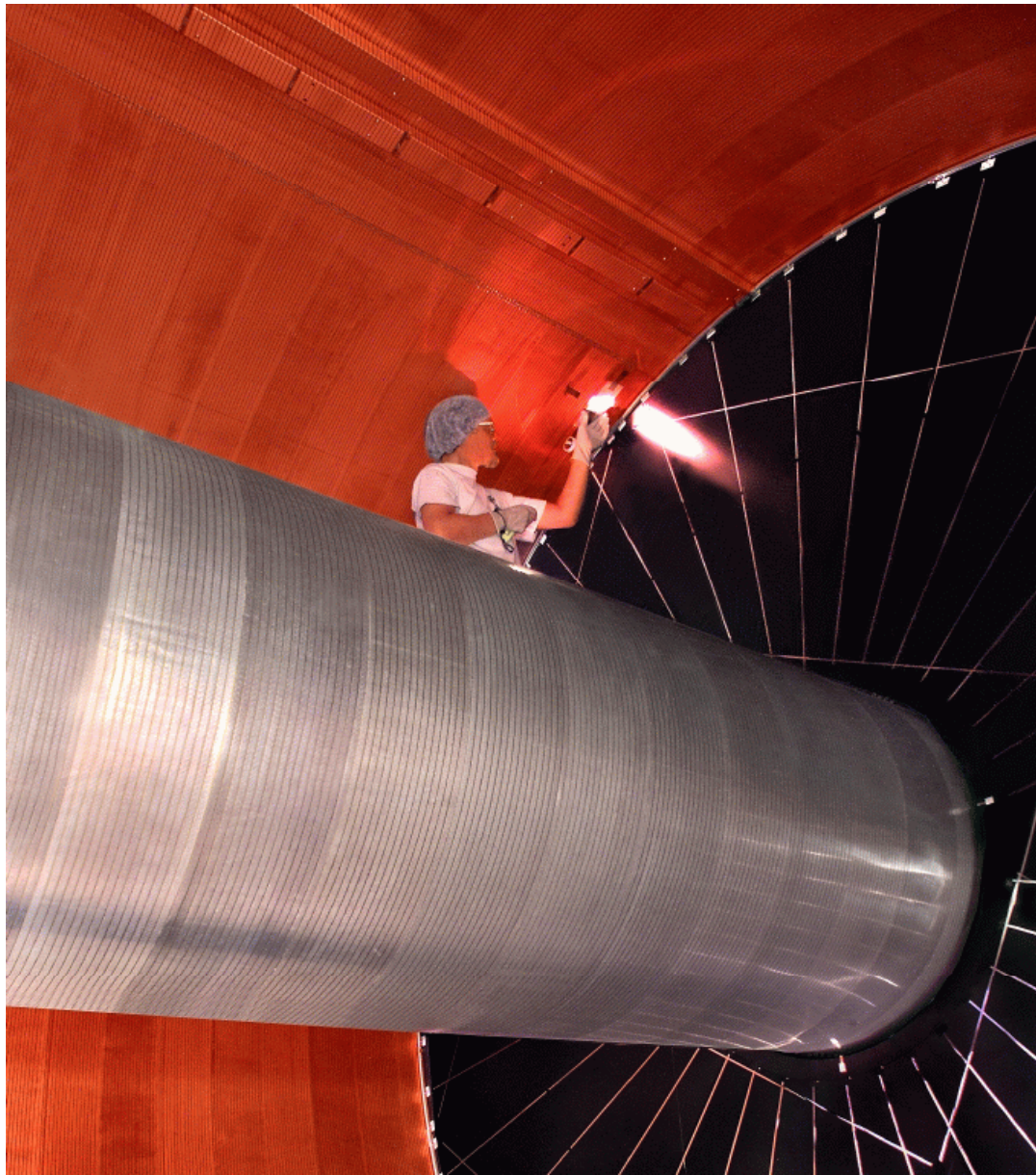


- energy loss in the tracking detectors (TPC dE/dx)
- time of flight measurement (TOF)
- calorimetric measurements (EMC)

STAR TPC Geometry



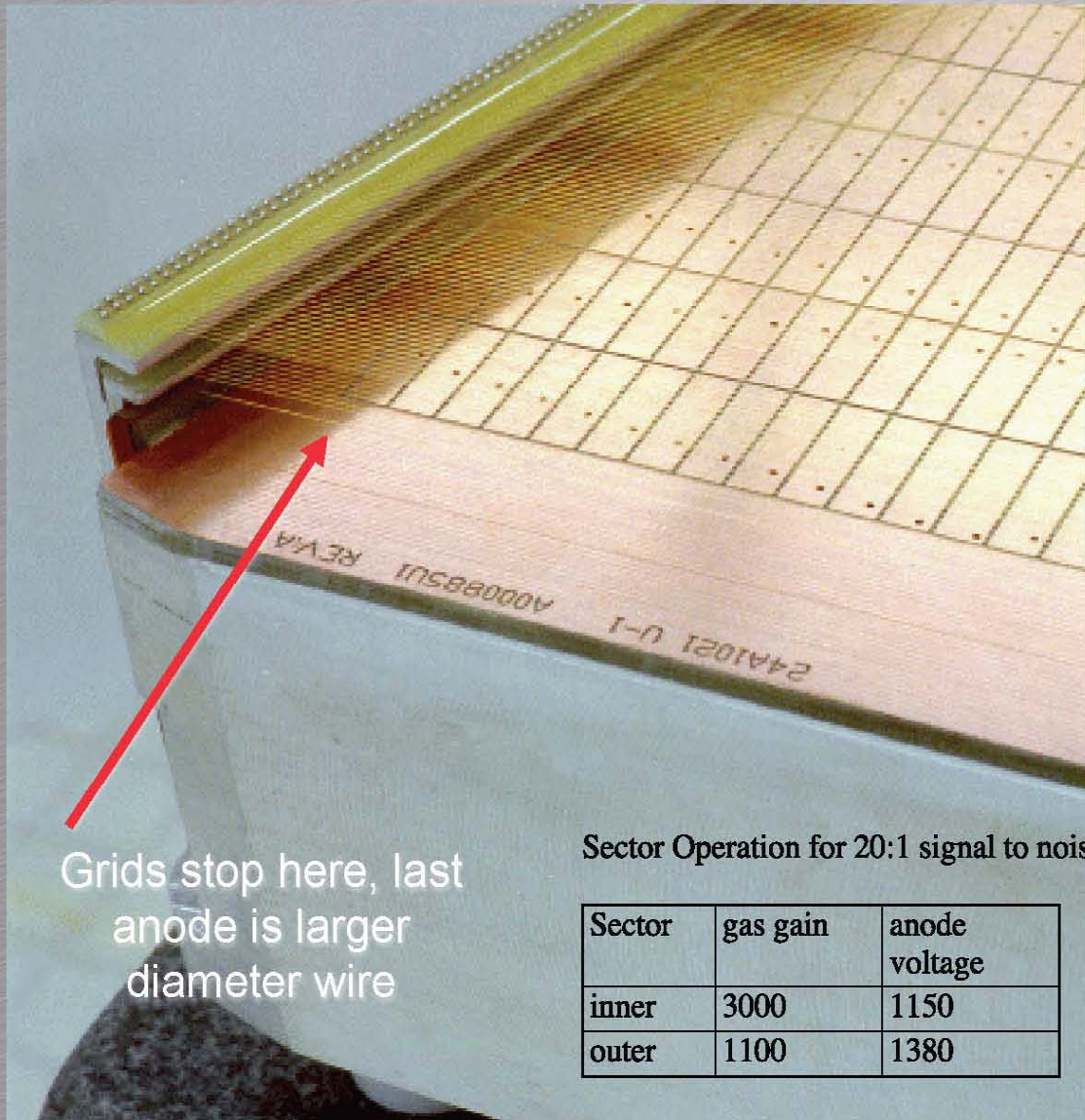
The STAR Time Projection Chamber



**Inner and Outer Field
Cages**

Central Membrane

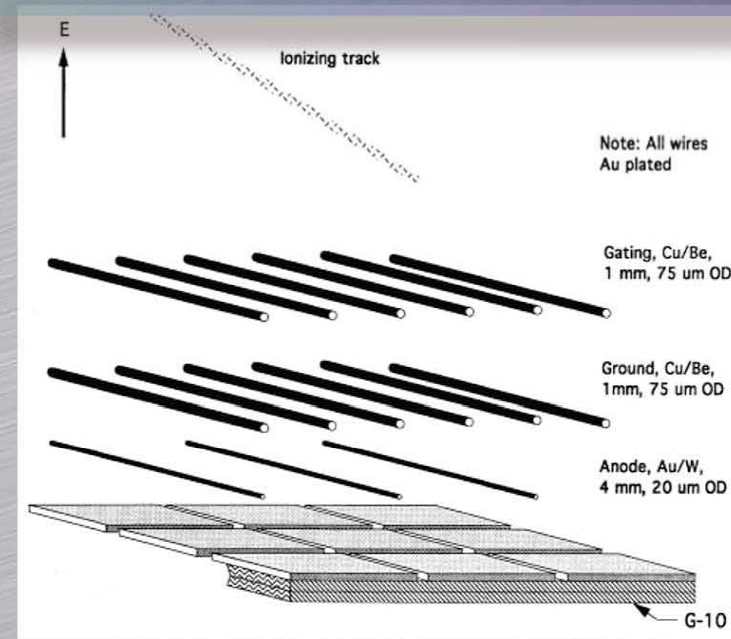
TPC Sector Detail



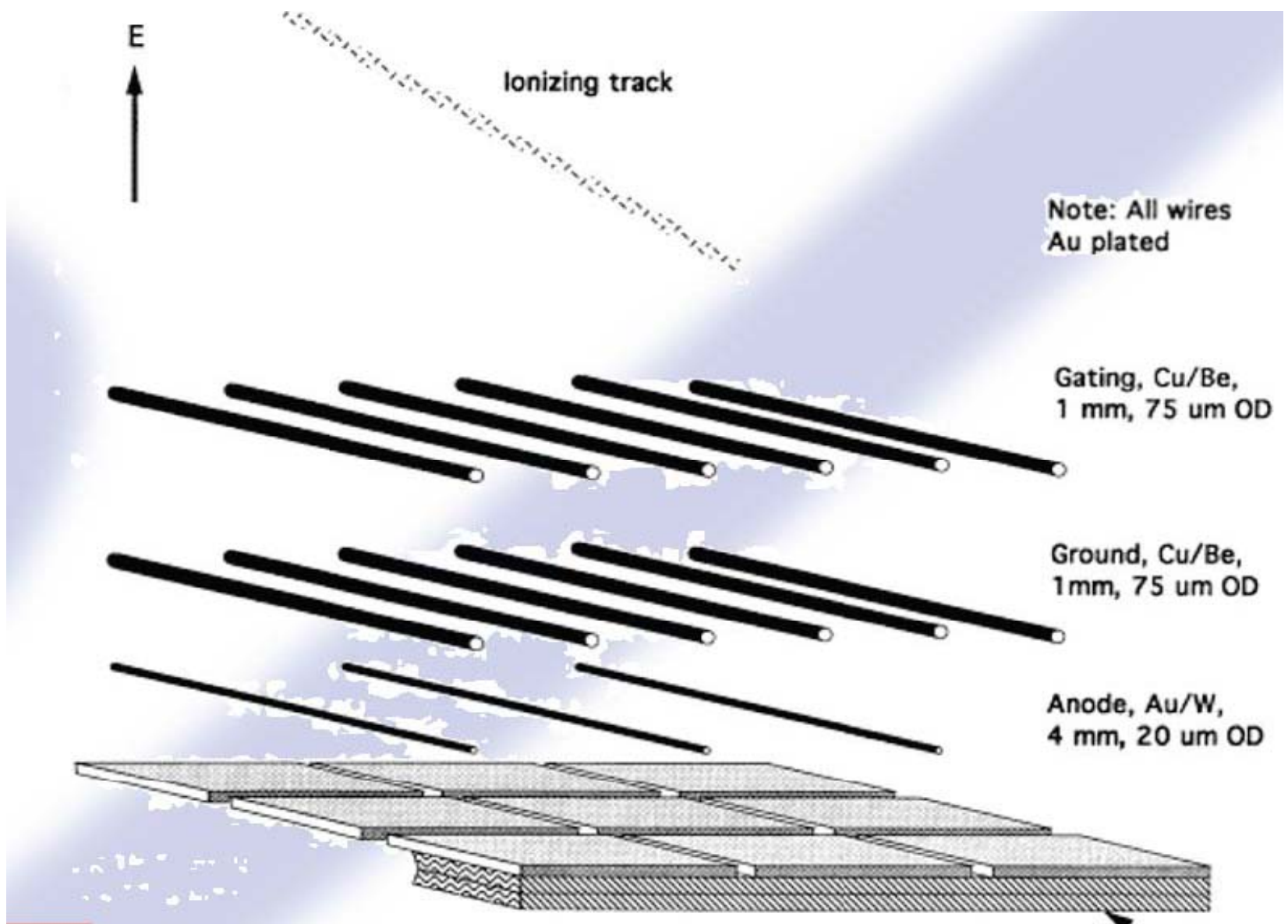
Sector Operation for 20:1 signal to noise

Sector	gas gain	anode voltage
inner	3000	1150
outer	1100	1380

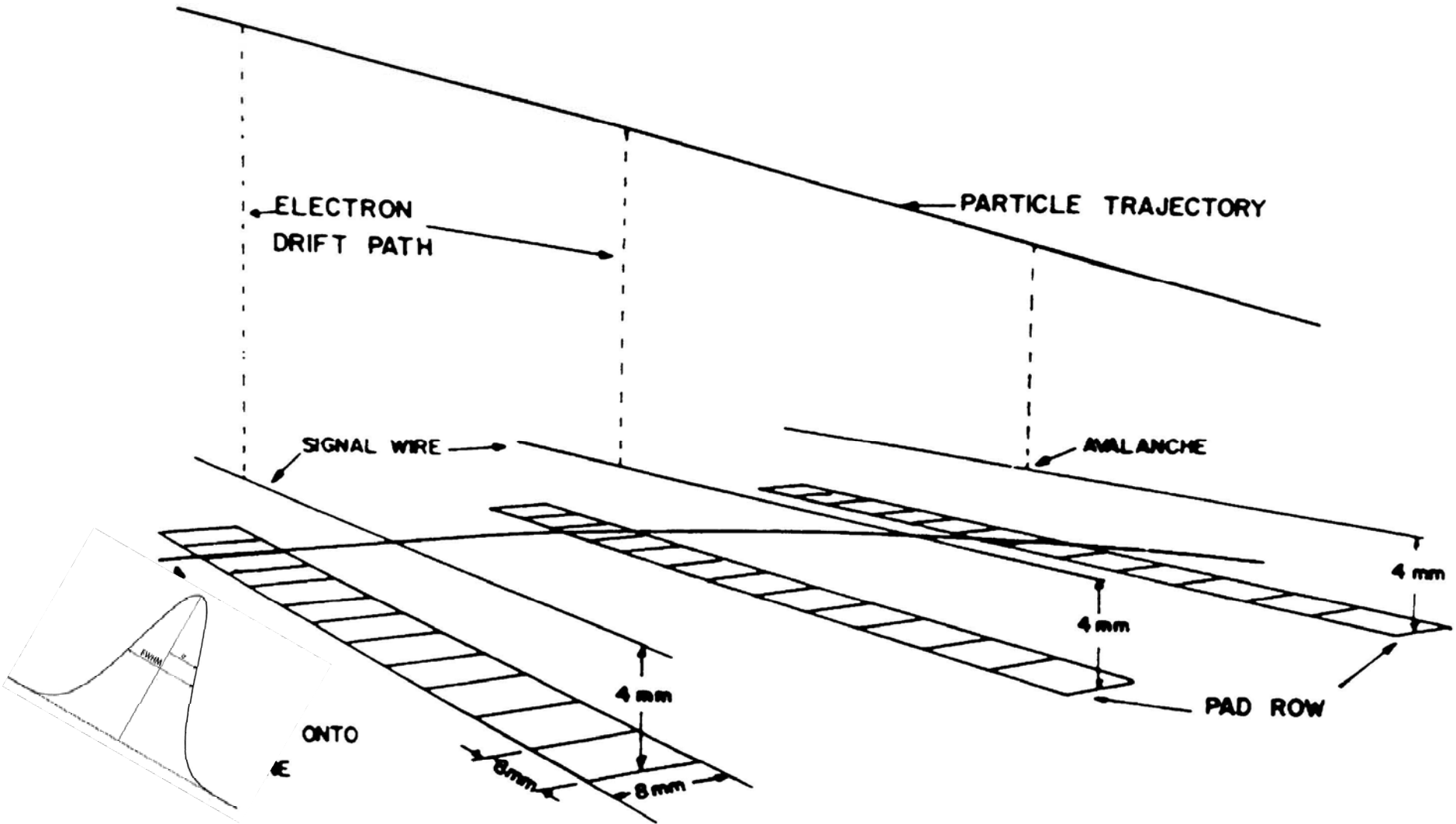
- Gating Grid
- Ground Plane of Wires
- Anodes
- No field shaping wires
- Simple and reliable
- Individually terminated anode wires limit cross-talk
- Low gain



Anode Wire-Plane Readout



Typical TPC Readout

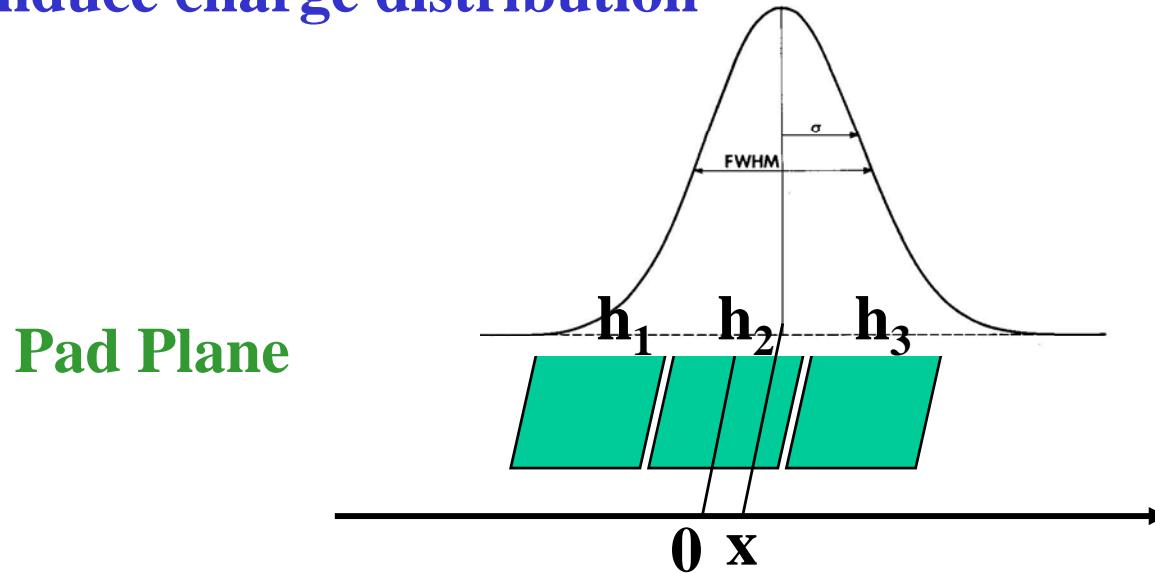


Limitations on Wire-Pad Readout

- 1) The induced charge distribution on the pad plane is much wider than the intrinsic avalanche width
 - wire-pad readout scheme not matching the true two-hit resolution capability of the gas detector
- 2) The width of the induced charge distribution depends on the separation between the anode and pad planes
 - STAR inner sectors 2 mm gap
 - outer sectors 4 mm gap
- 3) Mechanical stability and wire plane accuracy limit the gap separation
- 4) In high multiplicity environment the anode wire readout is not very useful

Hit Position from Pad Readout

Induce charge distribution



Ideally the induced signal should be distributed across three pads with amplitudes h_1 , h_2 and h_3 .

$$\sigma^2 = \frac{w^2}{\ln(h_2^2 / h_1 h_3)}$$

$$x = \frac{\sigma^2}{2w} \ln(h_3 / h_1)$$

**Non-Gaussian shape
better use weighted
average**

--- Laser signals

--- Drift direction

STAR TPC Characteristics

Item	Dimension	Comment
Length of the TPC	420 cm	Two halves, 210 cm long
Outer diameter of the drift volume	400 cm	200 cm radius
Inner diameter of the drift volume	100 cm	50 cm radius
Distance: cathode to ground plane	209.3 cm	Each side
Cathode	400 cm diameter	At the center of the TPC
Cathode potential	28 kV	Typical
Drift gas	P10	10% methane, 90% argon
Pressure	Atmospheric +2 mbar	Regulated at 2 mbar above atm.
Drift velocity	5.45 cm/ μ s	Typical
Transverse diffusion (σ)	230 μ m/ $\sqrt{\text{cm}}$	140 V/cm & 0.5 T
Longitudinal diffusion (σ)	360 μ m/ $\sqrt{\text{cm}}$	140 V/cm
Number of anode sectors	24	12 per end
Number of pads	136 608	
Signal to noise ratio	20:1	
Electronics shaping time	180 ns	FWHM
Signal dynamic range	10 bits	
Sampling rate	9.4 MHz	
Sampling depth	512 time buckets	380 time buckets typical

P10 Gas

Electrons Transport in Gas

Electron clouds from primary ionization drift towards the anode and undergo diffusion

D – diffusion coefficient

Under magnetic field (parallel to Electric Field **E**)
the transverse diffusion coefficient --

$$D_T(B) = \frac{D_T}{\sqrt{1 + (\omega\tau)^2}}$$

P10 Gas – $\omega\tau \sim 2.30$ at **0.5 T**

$$D_T(0.5T) = 230 \text{ } \mu\text{m}/\text{sqrt}(\text{cm})$$

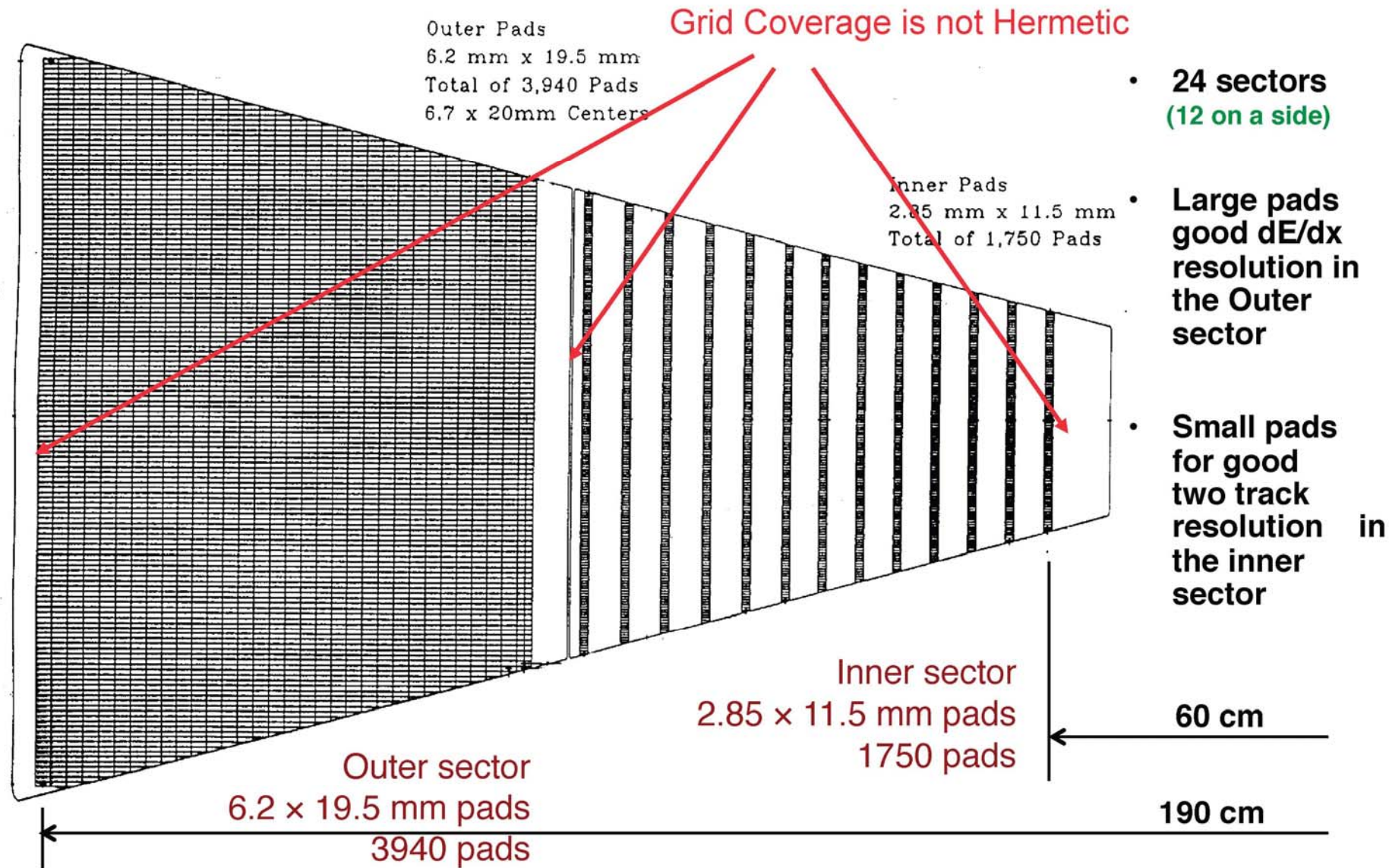
$$D_L = 360 \text{ } \mu\text{m}/\text{sqrt}(\text{cm})$$

Diffusion Contribution $\sigma \sim D \cdot \text{sqrt}(L)$

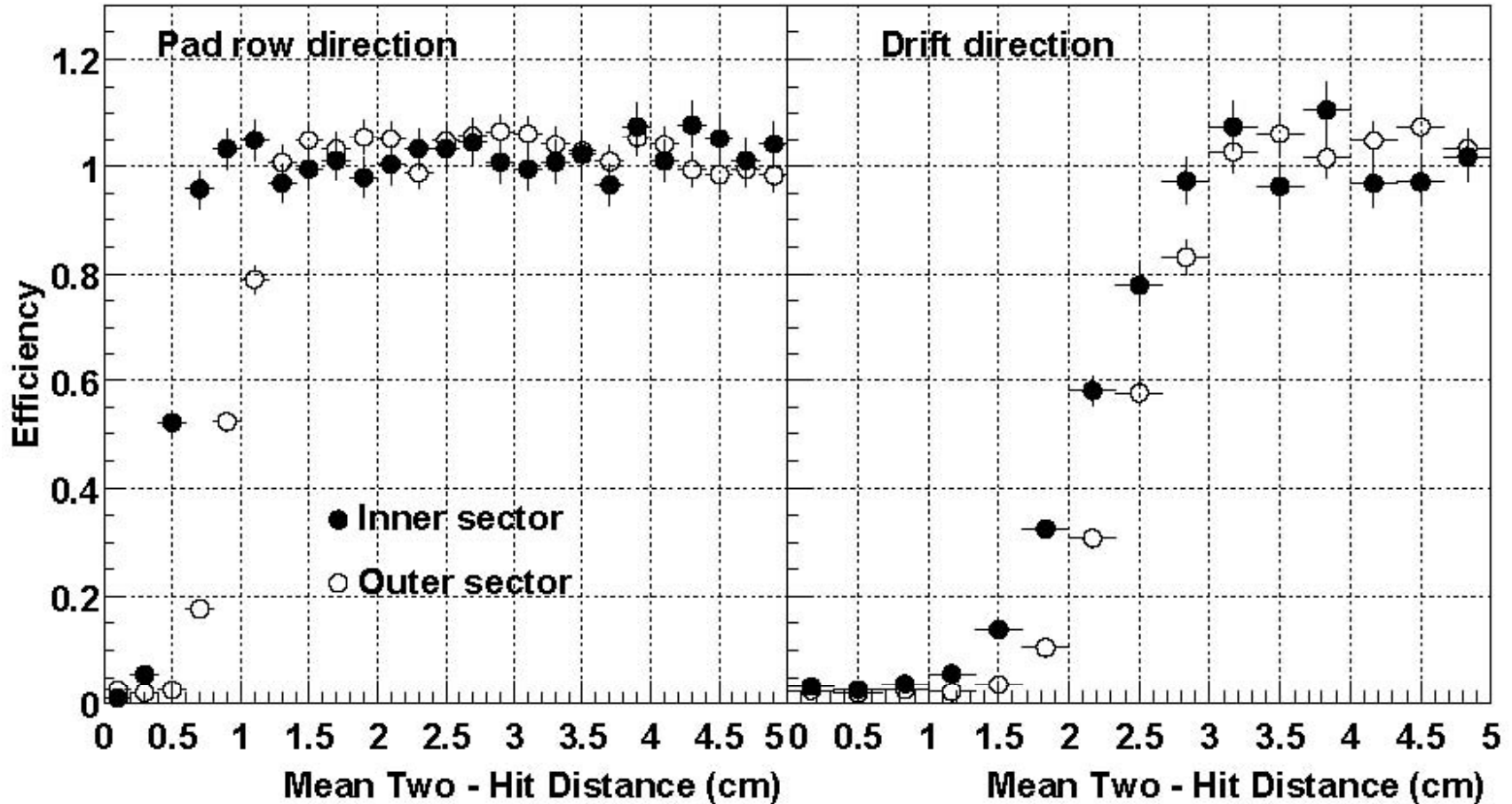
For **L=200 cm** drift in **STAR TPC** $\sigma_T \sim 3.3 \text{ mm}$; $\sigma_L \sim 5.1 \text{ mm}$

-- **Anode Wire – Pad Plane two-hit resolution does not match the diffusion limit – motivation for GEM read-out !!**

Outer and Inner Sectors of the Pad Plane



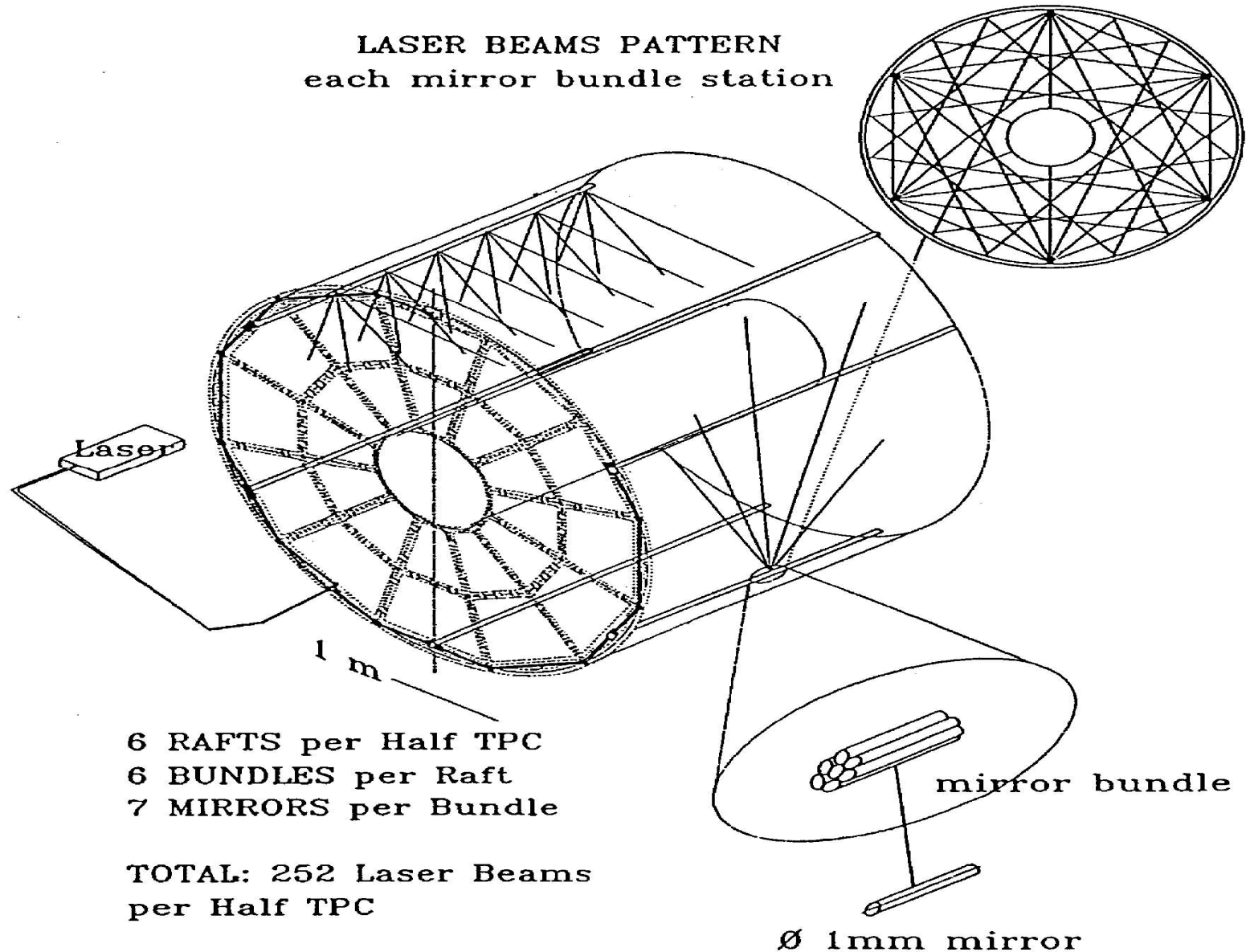
Two-Hit Resolutions



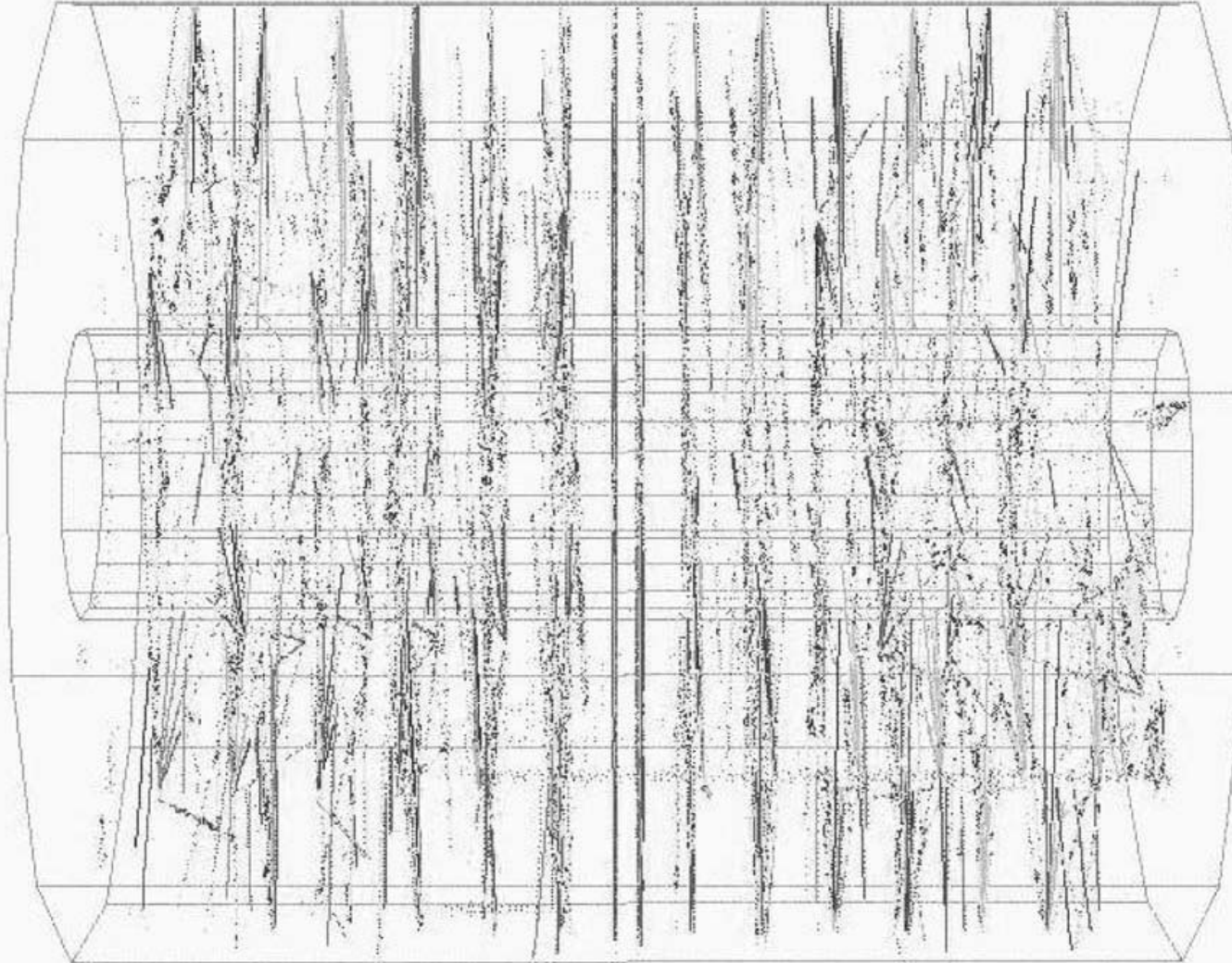
Inner Sector Pads – 2.85 x 11.5 mm

Outer Sector Pads – 6.20 x 19.5 mm

Laser System for Drift Velocity



TPC Laser Tracks

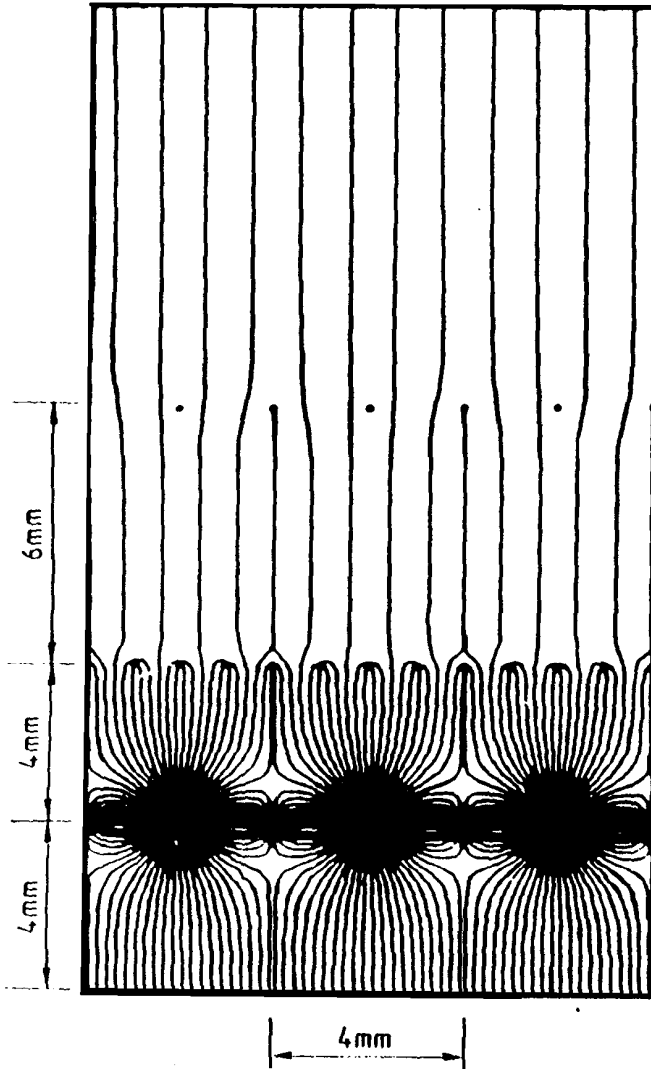


Laser System

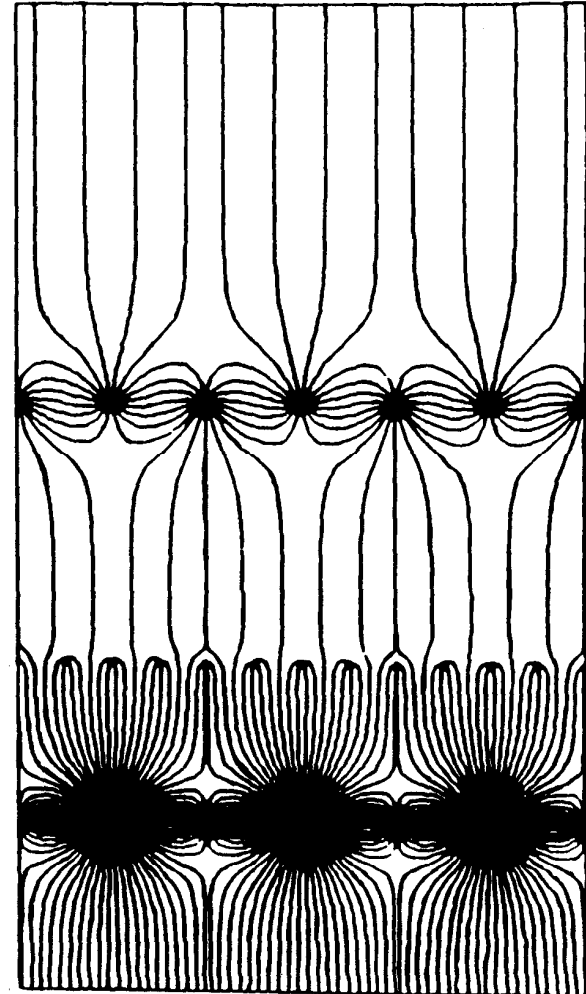
- 500 laser triggers every a few hours !
- drift velocity $\sigma \sim 0.02\%$

What Happens to Positive Ions?

Gate open



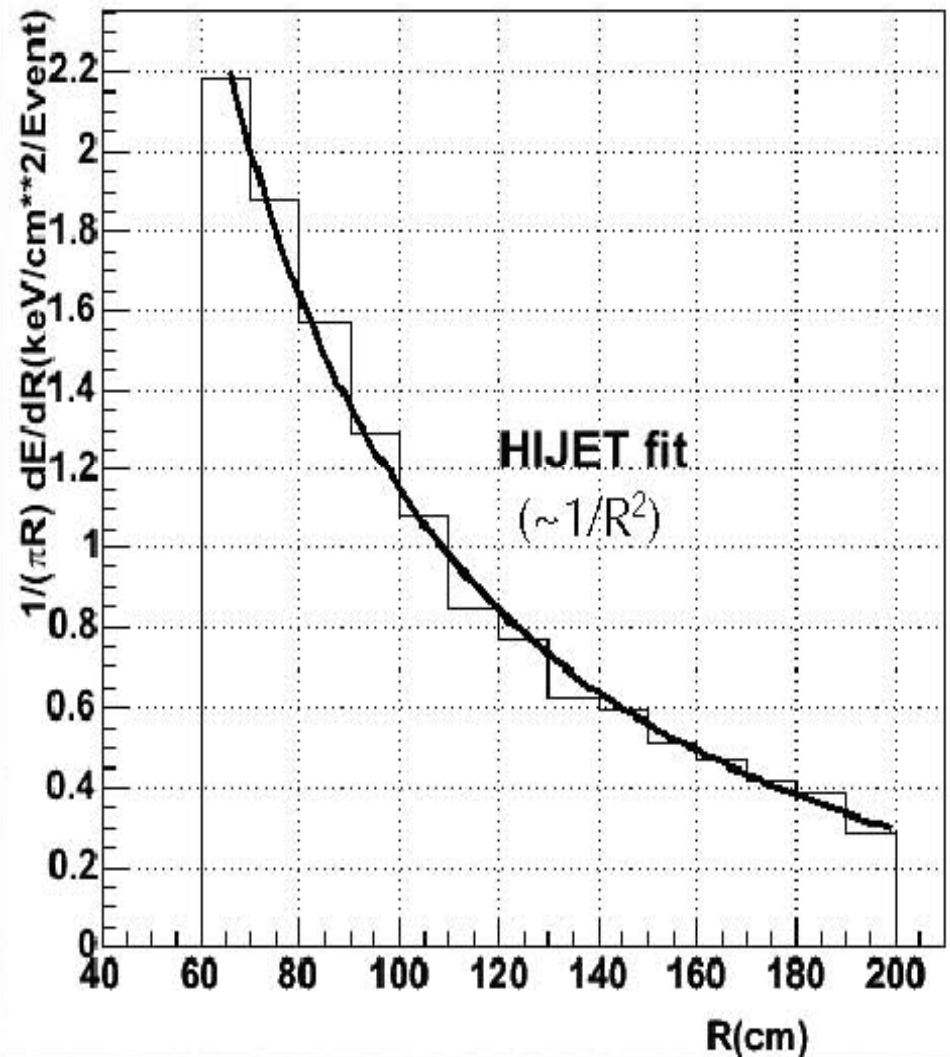
Gate closed



SpaceCharge: model of charge

HIJET model of “event shape” for 200 GeV AuAu collisions matches radial distribution of zerobias data well for much of the runs.

Radial distribution of TPC SpaceCharge



Distortion equations

(see Blum & Rolandi)

Solve:

$$m \frac{d\bar{u}}{dt} = e\bar{E} + e[\bar{u} \times \bar{B}] - K\bar{u}$$

Langevin Equation with "Friction"

substituting:

$$\tau = \frac{m}{K}, \quad \omega = \frac{e}{m} |\bar{B}|, \quad \mu = \frac{e}{m} \tau, \quad \text{and} \quad \hat{E} = \frac{\bar{E}}{|\bar{E}|}$$

subject to the
steady state
condition

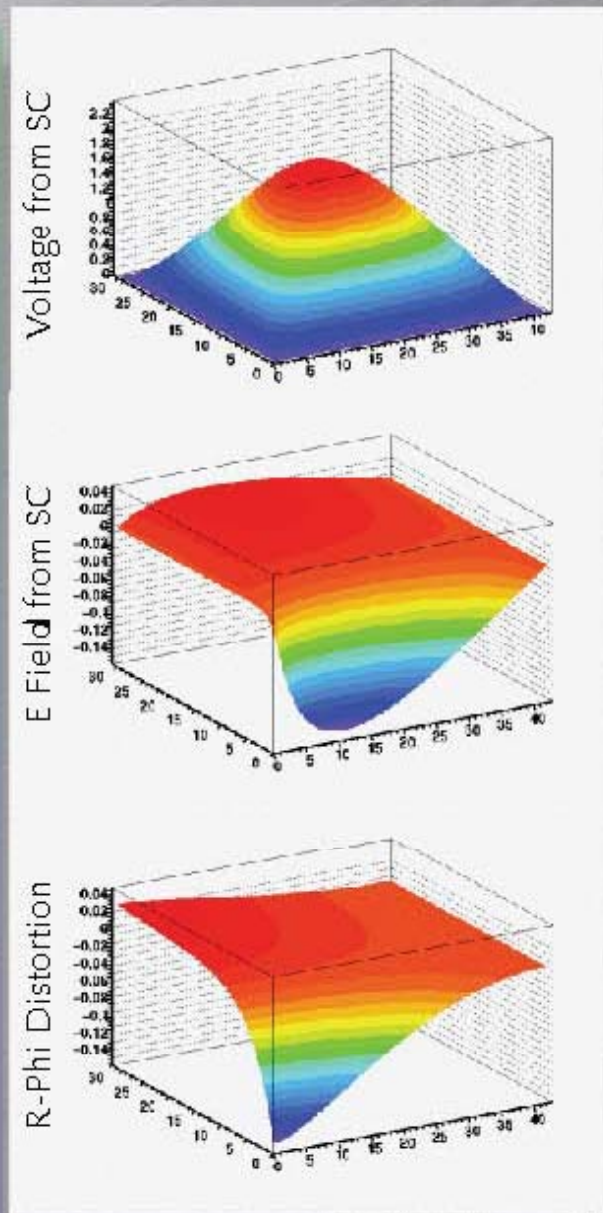
$$\frac{d\bar{u}}{dt} = 0 \quad \text{yields}$$

$$\bar{u} = \frac{\mu |\bar{E}|}{(1 + \omega^2 \tau^2)} \left(\hat{E} + \omega \tau [\hat{E} \times \hat{B}] + \omega^2 \tau^2 (\hat{E} \cdot \hat{B}) \hat{B} \right)$$

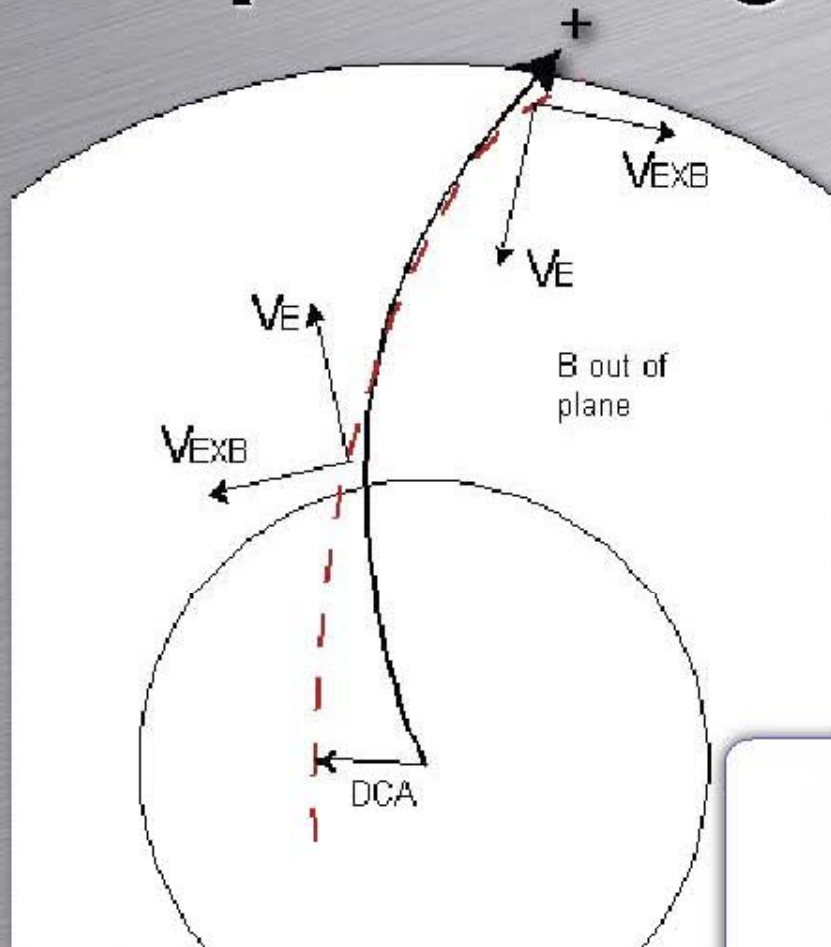
Large Data Set is needed for correction studies !

SpaceCharge Field Effects

- Using our “event shape” model
 - Relaxation done on 5cm x 5cm 2D (r-z) grid (assume Φ symmetry)
 - Treat as a perturbation on top of standard TPC E field
 - Distortions are integral of E field in z (drift direction)
 - Not very sensitive to radial component of distortion because tracks are radial-like
- Lorentz Force Eqn: $\vec{F} \propto q \cdot (\vec{E} \times \vec{B})$

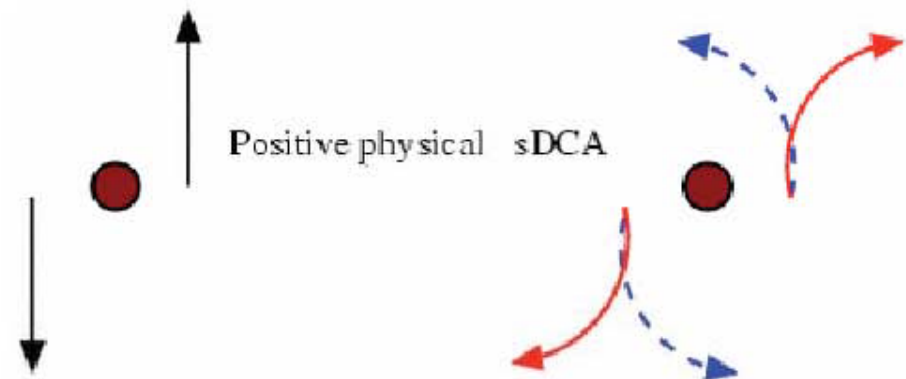


SpaceCharge effect on sDCA

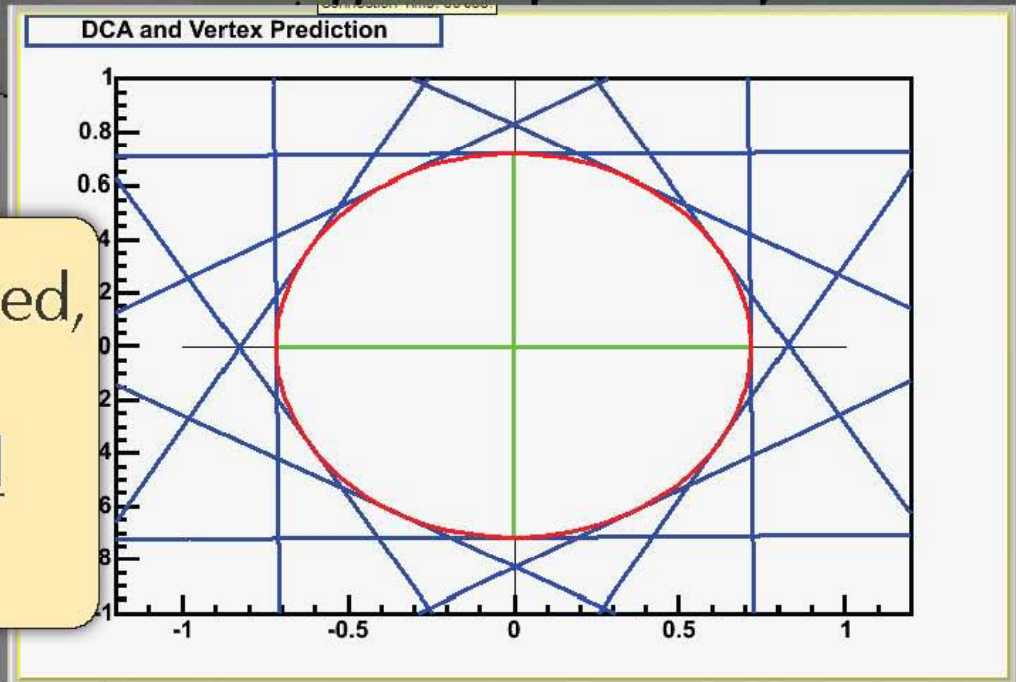


- All tracks go the same direction (pos. or neg.)
- Track charge independence
- Field dependence

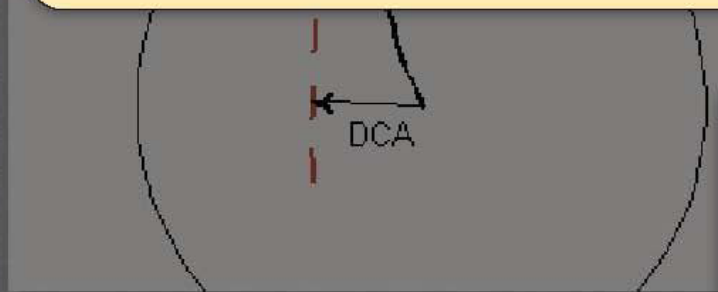
sDCA = signed distance of closest approach



SpaceCharge effect on sDCA



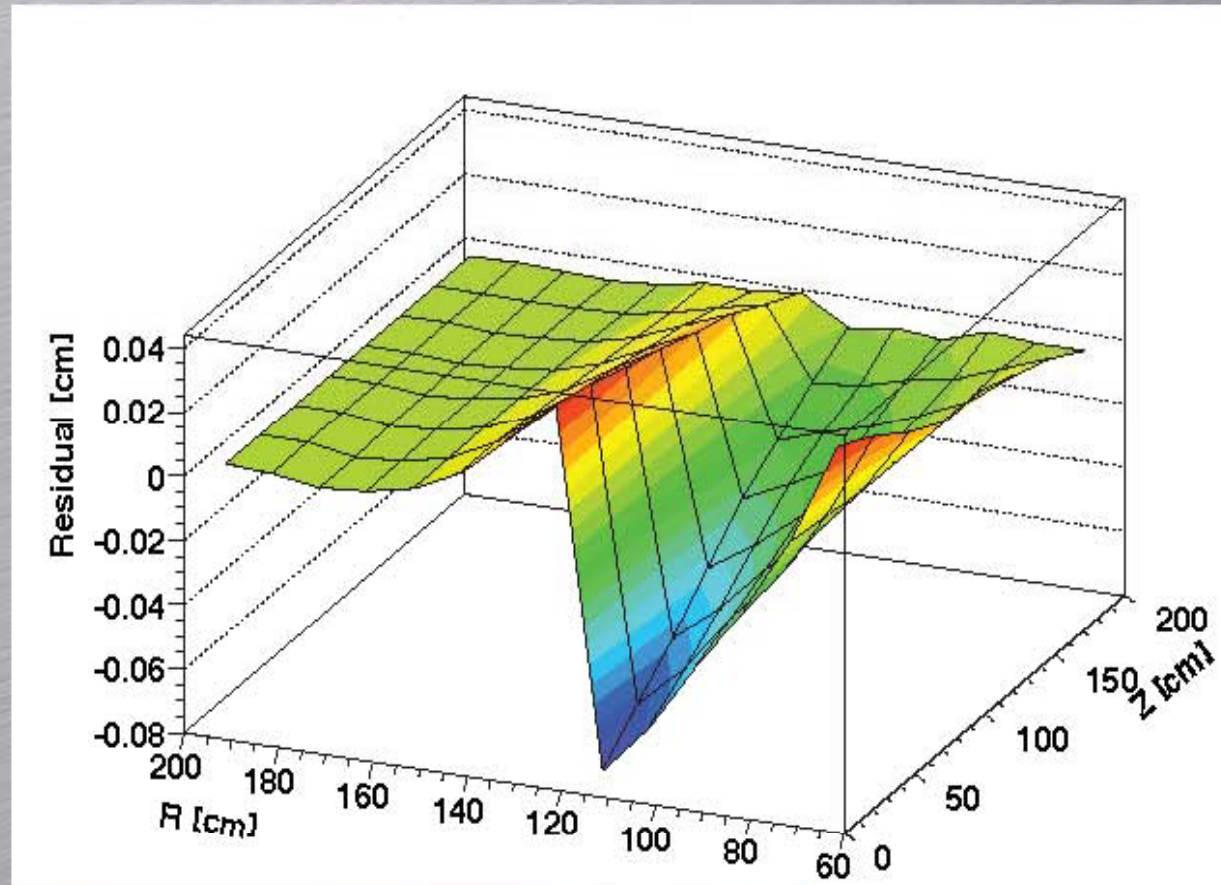
Vertex-finding de-focused,
but not biased:
vertex makes a good
reference point



sDCA = signed distance
of closest approach



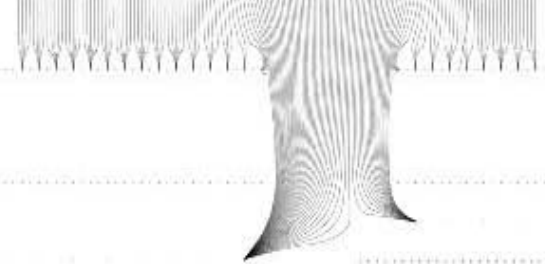
TPC GridLeak distortion



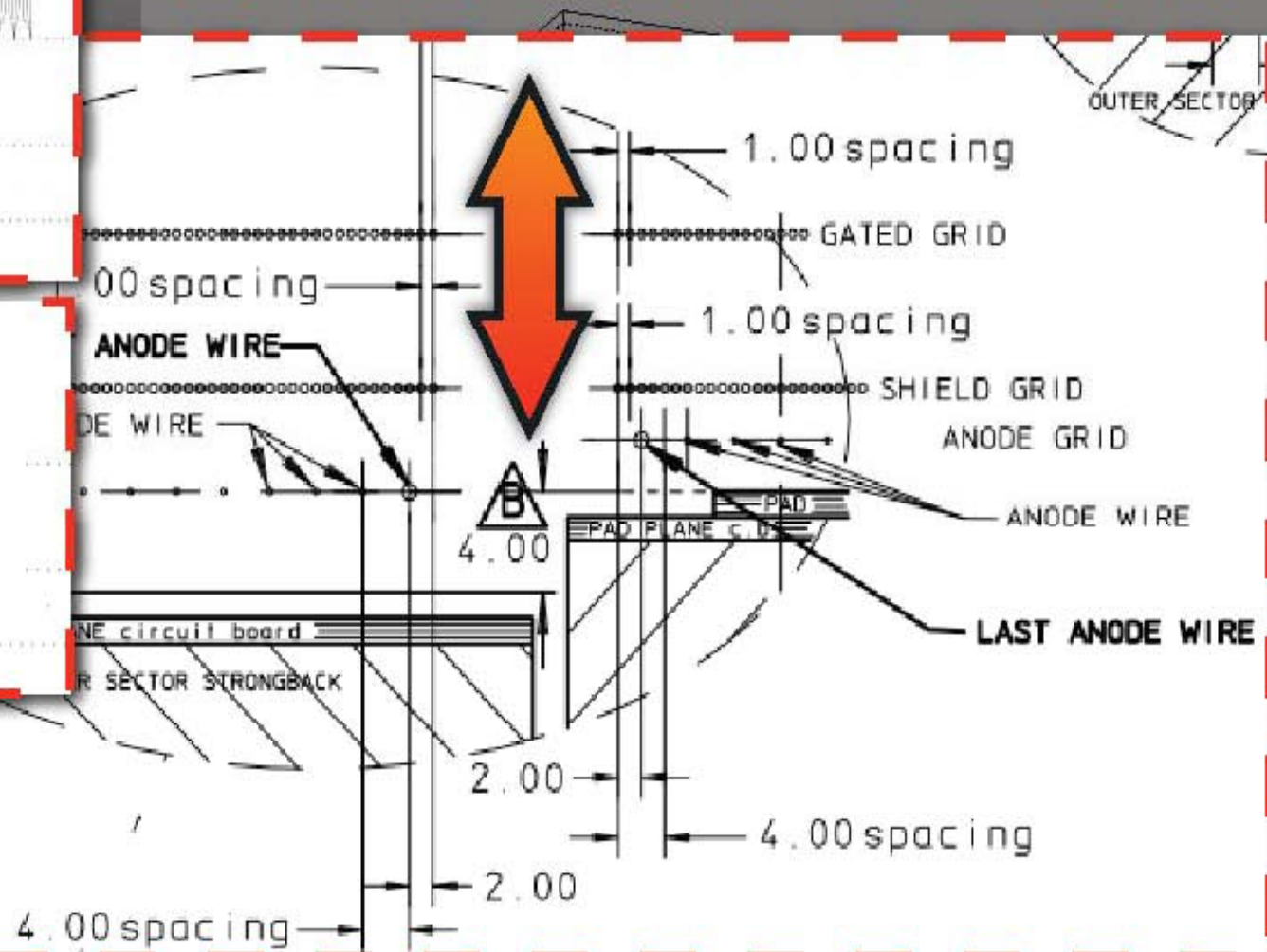
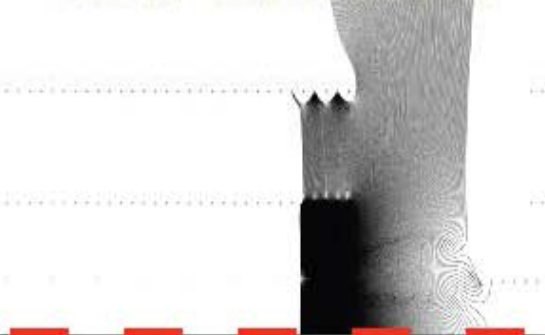
- Dependence on field, track charge, location, luminosity consistent with ion leakage at gating grid gap

TPC GridLeak distortion

Electrons inbound



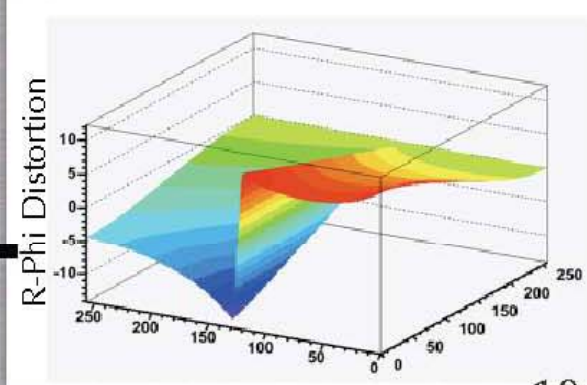
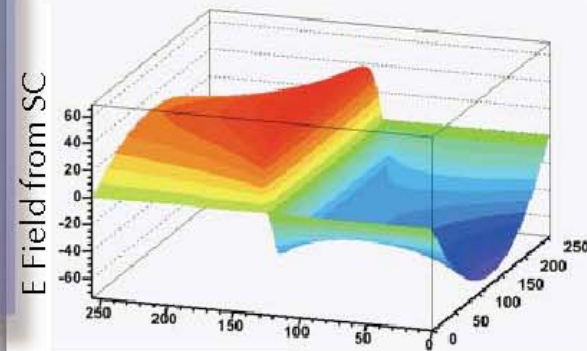
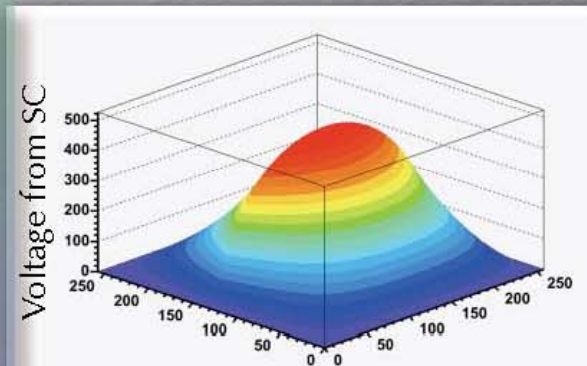
Ions outbound



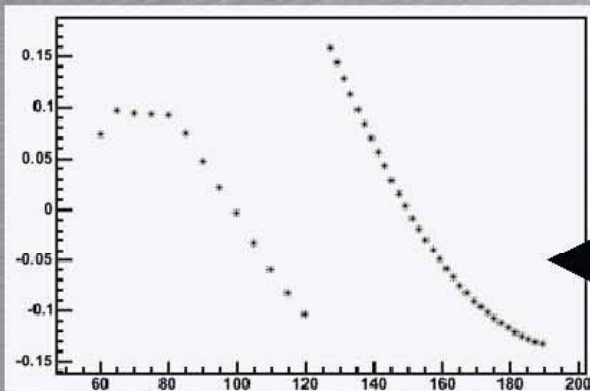
ion leakage at gating grid gap

GridLeak Field Effects

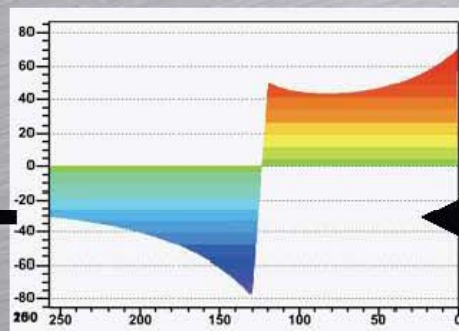
- Modeled sheets of charge
 - Relaxation done on custom 3D grid (plots assume Φ symmetry, but leak is 12-fold symmetry from grid shape)
 - E-field and distortion discontinuity at grid gap
- GridLeak scales as SpaceCharge!



Simulated residuals on a track



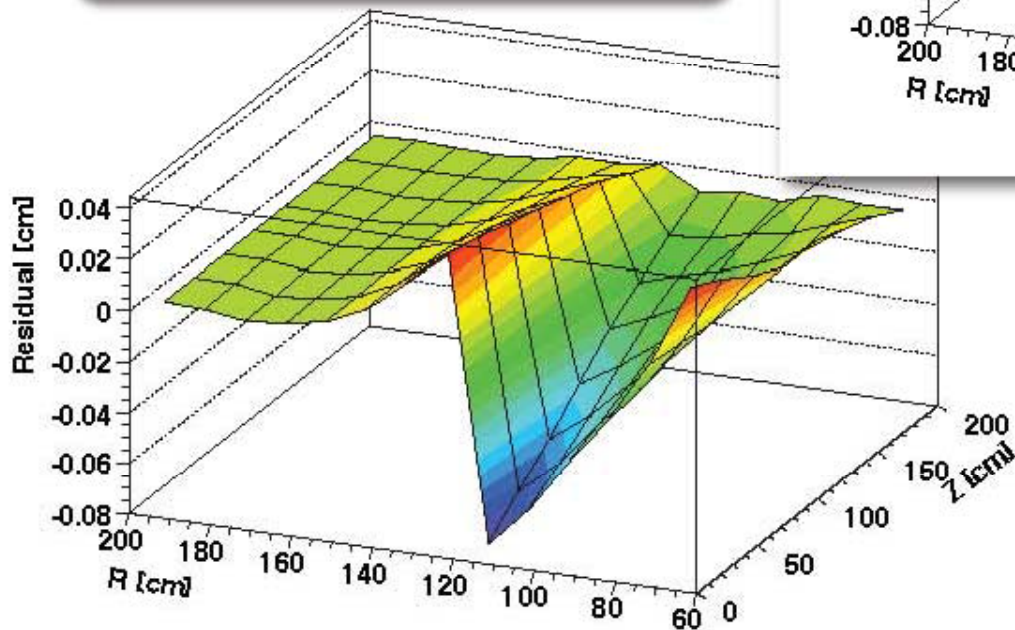
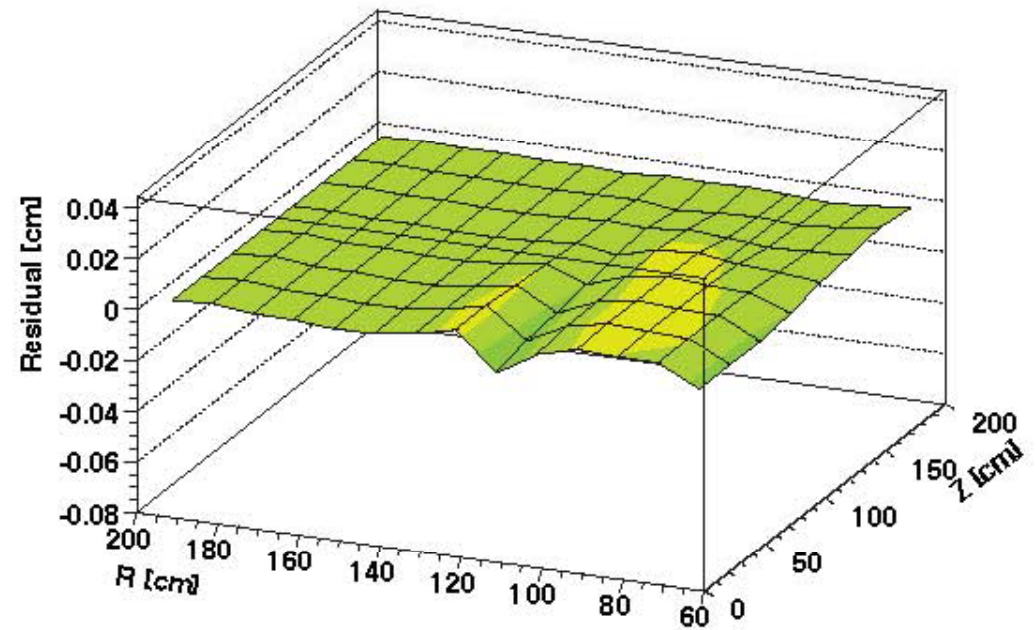
Distortion near CM



Applied GridLeak Correction

- Not perfect, but as good as design spec!

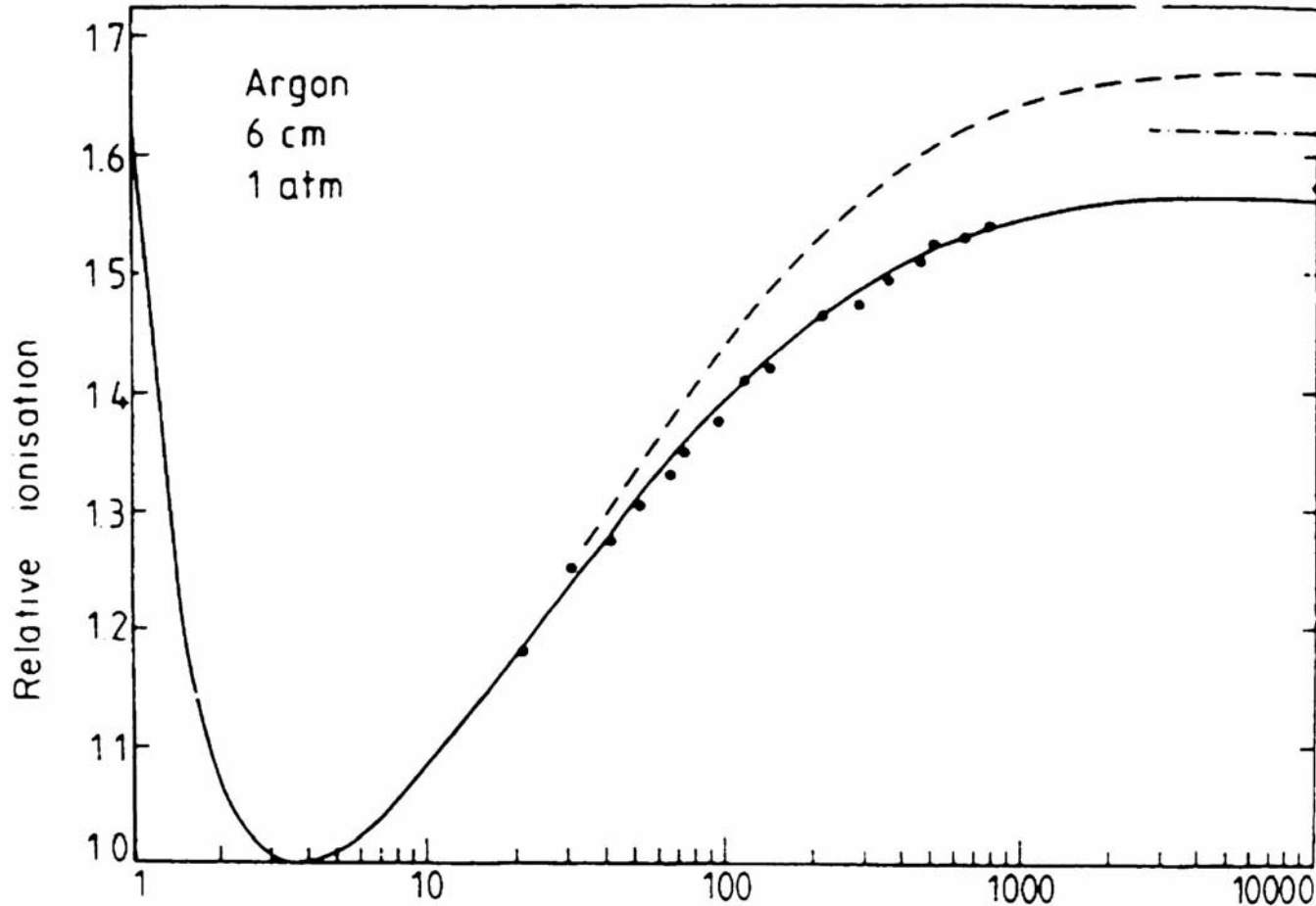
Distortions scale significantly reduced!



After

Before

Ionization Energy



Bethe-Bloch Formula

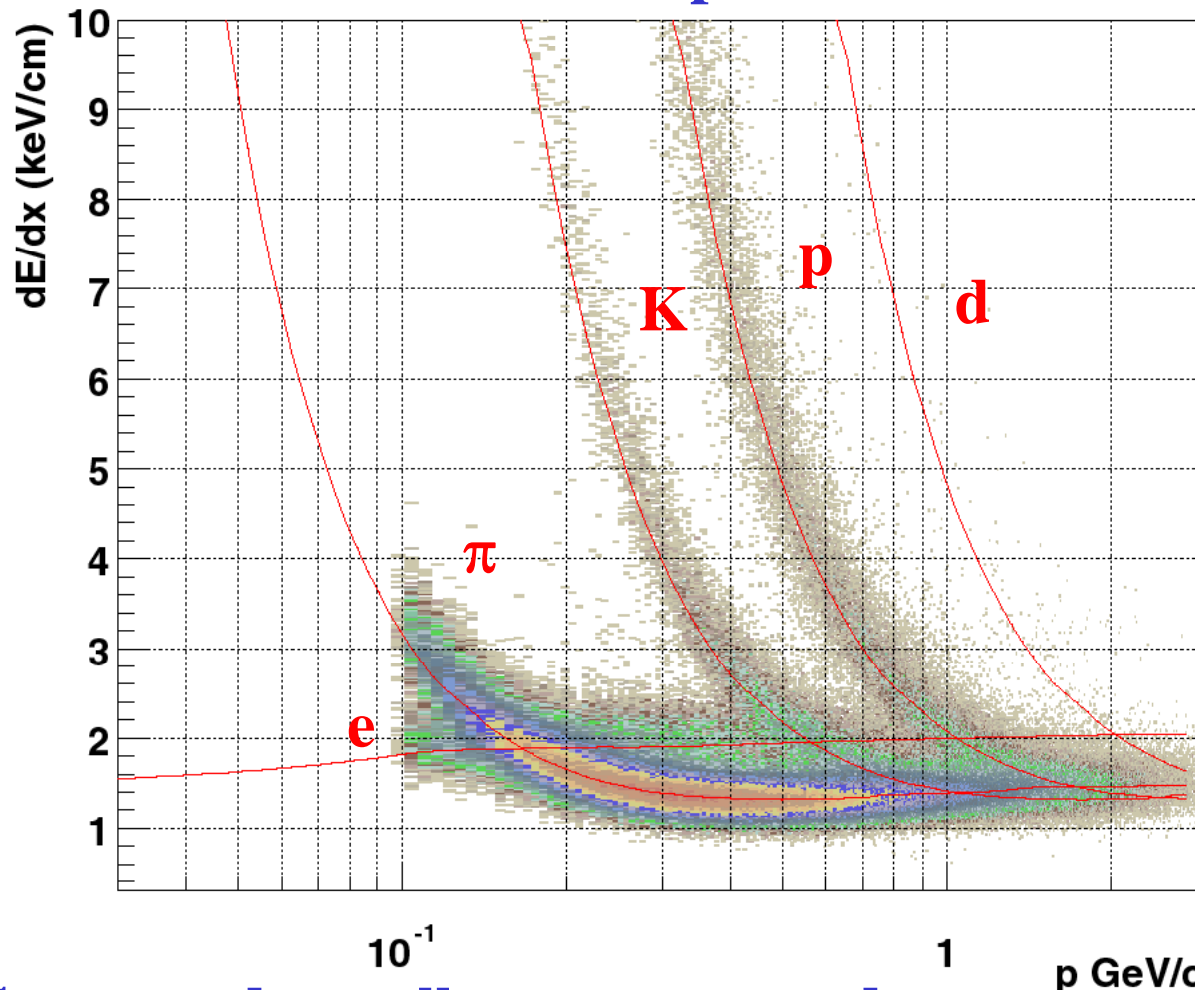
$$\left\langle \frac{dE}{dx} \right\rangle = -4\pi N_A r_e^2 m_e c^2 z^2 \frac{Z}{A} \frac{1}{\beta^2} \left[\ln \left(\frac{2m_e c^2 \gamma^2 \beta^2}{I} \right) - \beta^2 - \frac{\delta}{2} \right]$$

density effect

ionization constant

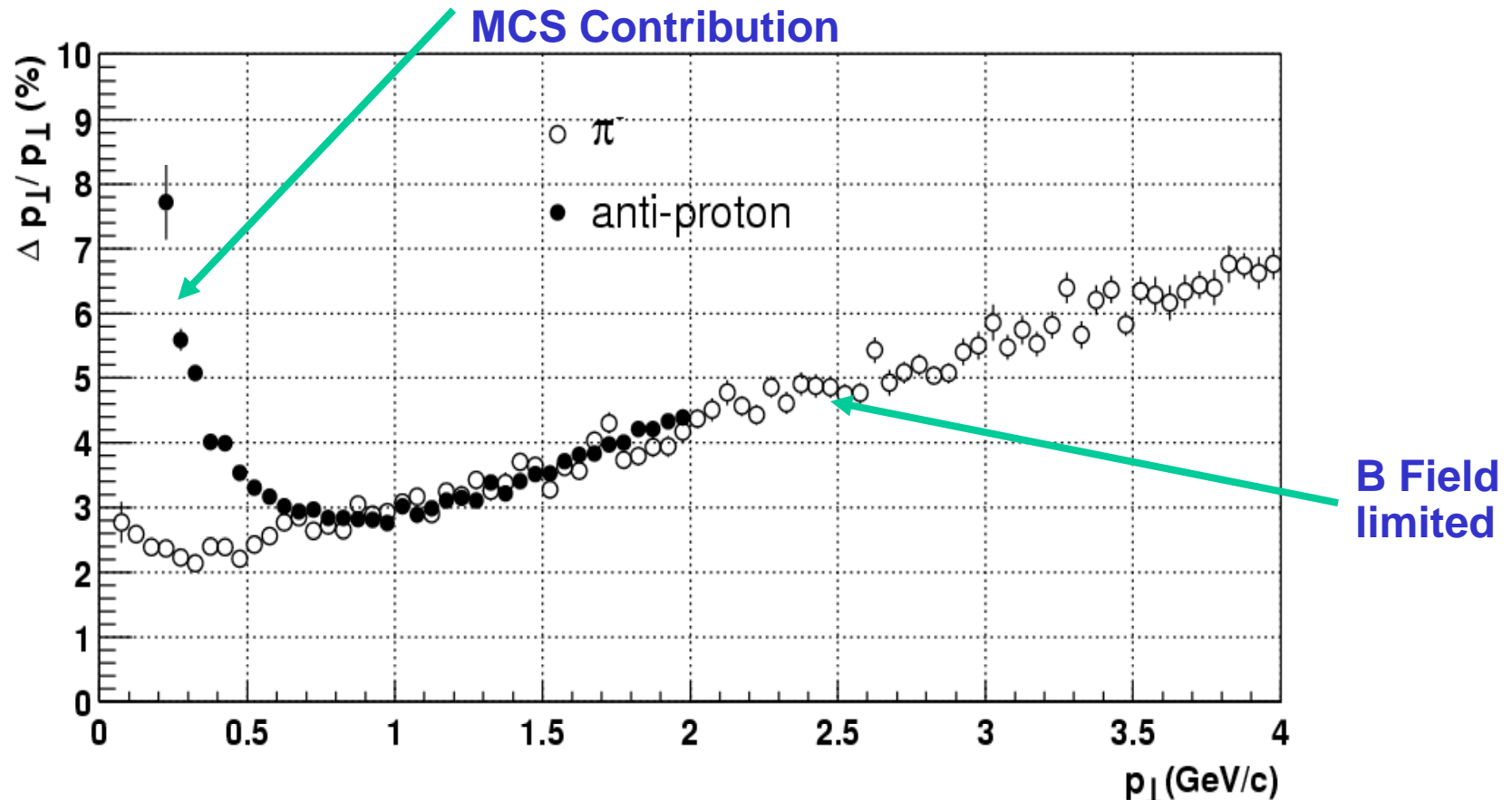
Particle Identification Using dE/dx

STAR TPC: Ar-CH₄ (90-10) Atmosphere Pressure
45 max samples



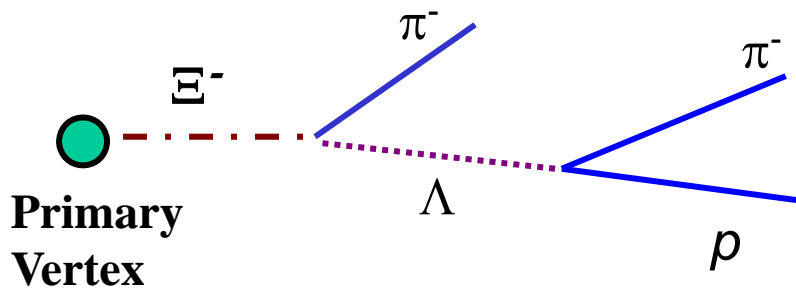
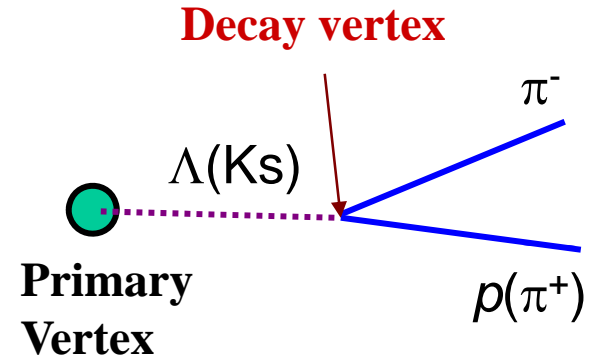
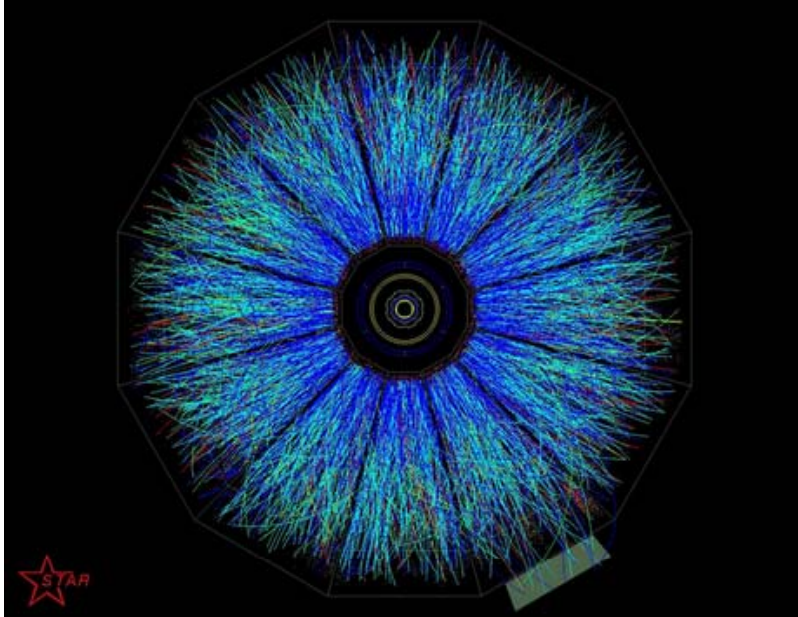
Inner Sector pads smaller – not as good as outer pads for dE/dx

Momentum Resolution: the STAR Magnet+TPC



- Momentum resolution is only limited by the strength of the magnetic field and is independent of the mass of the particle at high P_T
- Momentum resolution at low P_T is determined by multiple coulomb scattering (MCS)

Reconstruct K_S , Λ and Ξ



$$K_S \rightarrow \pi^+ \pi^- \quad (\Gamma_i/\Gamma \approx 69\%), \quad c\tau = 2.69\text{cm}$$

$$\Lambda \rightarrow p \pi \quad (\Gamma_i/\Gamma \approx 64\%), \quad c\tau = 7.89\text{cm}$$

$$\Xi^- \rightarrow \Lambda \pi \quad (\Gamma_i/\Gamma \approx 99.9\%), \quad c\tau = 4.91\text{cm}$$

$$m = \sqrt{(\sqrt{m_+^2 + P_+^2} + \sqrt{m_-^2 + P_-^2})^2 - P^2},$$

STAR TPC

The STAR TPC has performed as designed

-- unexpected space-charge problem

**due to higher RHIC luminosity ~ 6 x design luminosity
some charge leakage in the gating grid boundary
can be corrected for reliably so far**

STAR benefited from

- 1) better than design spec on construction and E and B alignment**
- 2) TPC has two almost independent halves (central membrane)**
- 3) many monitor systems and lots of data**

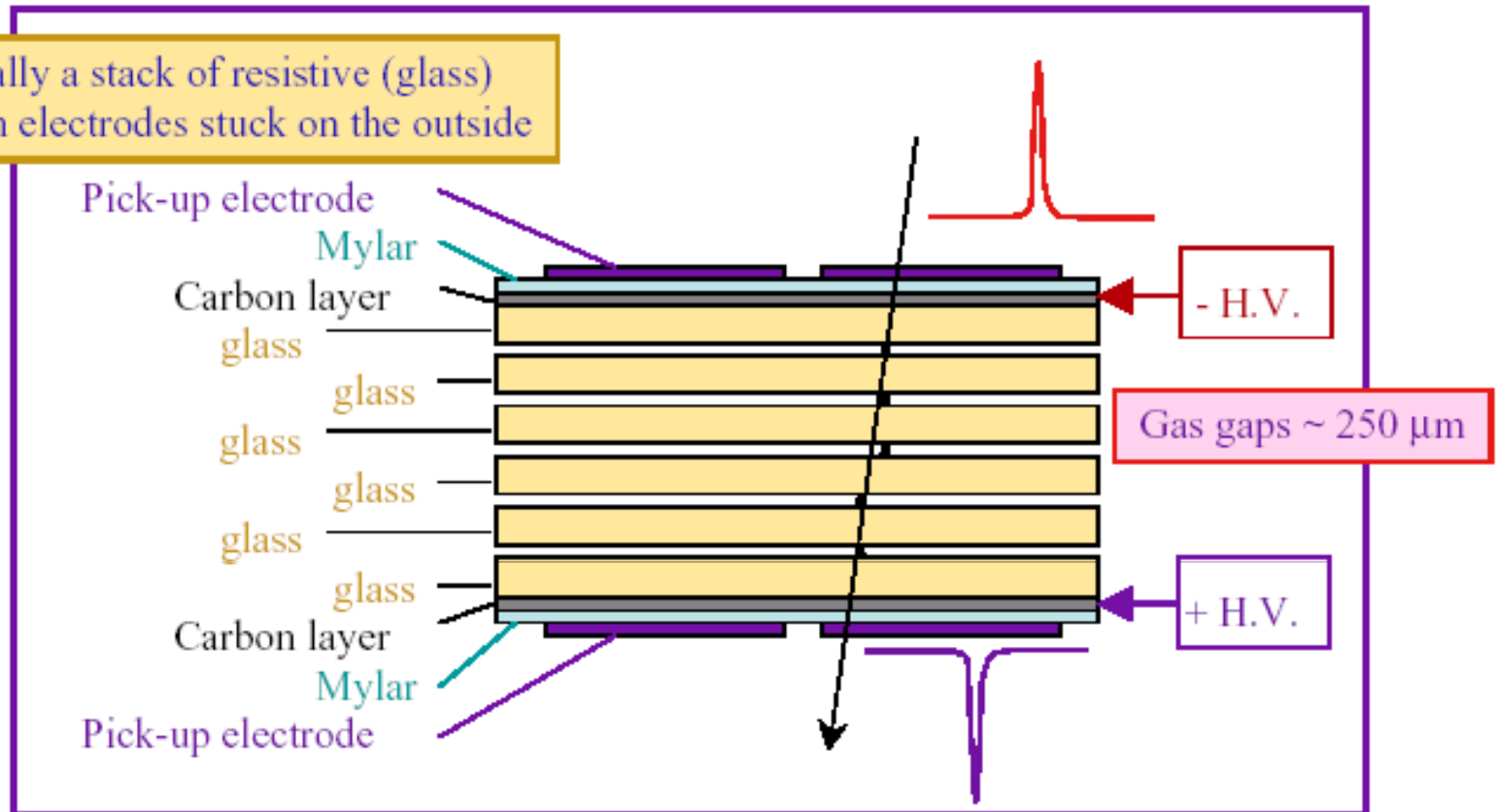
STAR TPC upgrade – FEE and DAQ

STAR TPC is expected to perform at RHICII @40 x design L

Multi-Gap Resistive Plate Chamber

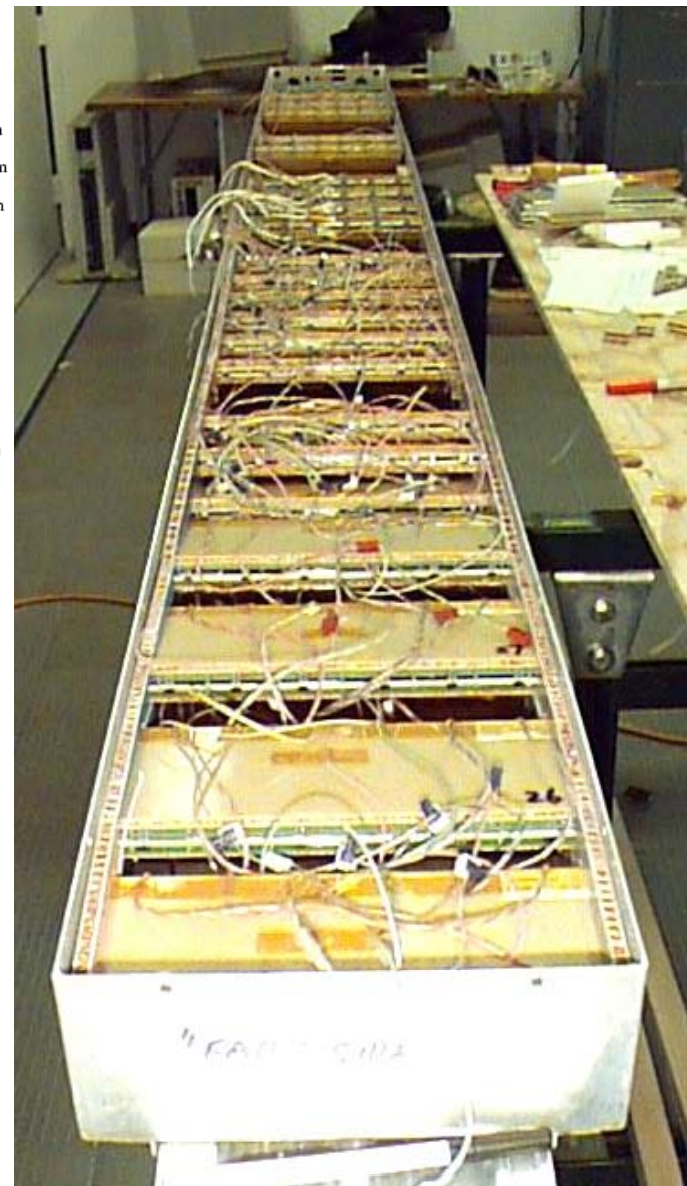
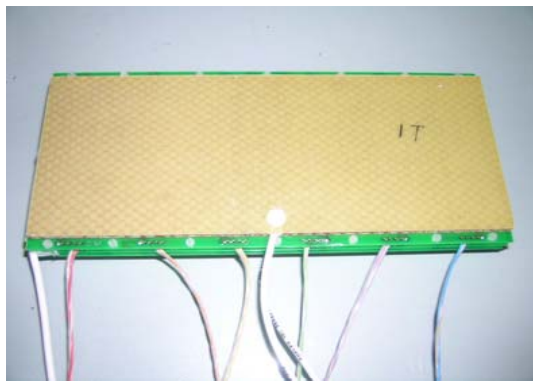
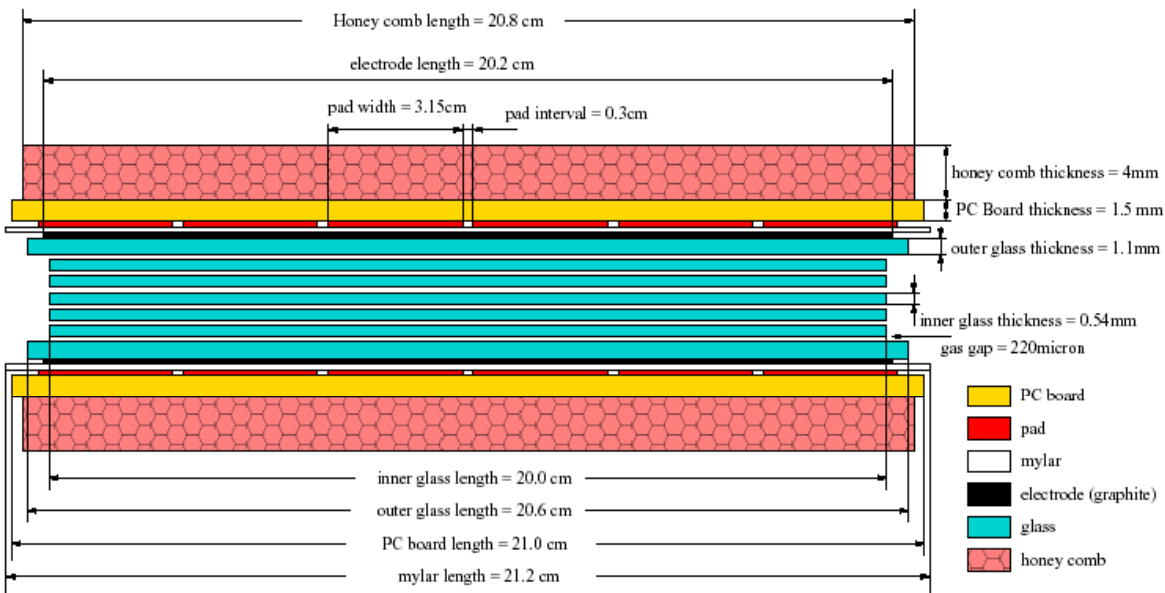
The MULTIGAP Resistive Plate Chamber

Essentially a stack of resistive (glass) plates with electrodes stuck on the outside



Note 1: internal glass plates electrically floating - take and keep correct voltage by electrostatics and flow of electrons and ions produced in gas avalanches

Note 2: resistive plates transparent to fast signals - induced signals on external electrodes is sum of signals from all gaps



Good time resolution ($< 100\text{ps}$),
 high detection efficiency ($> 95\%$),
 high granularity, robustious,
 low cost (\$2M + electronic).

USTC and Tsinghua

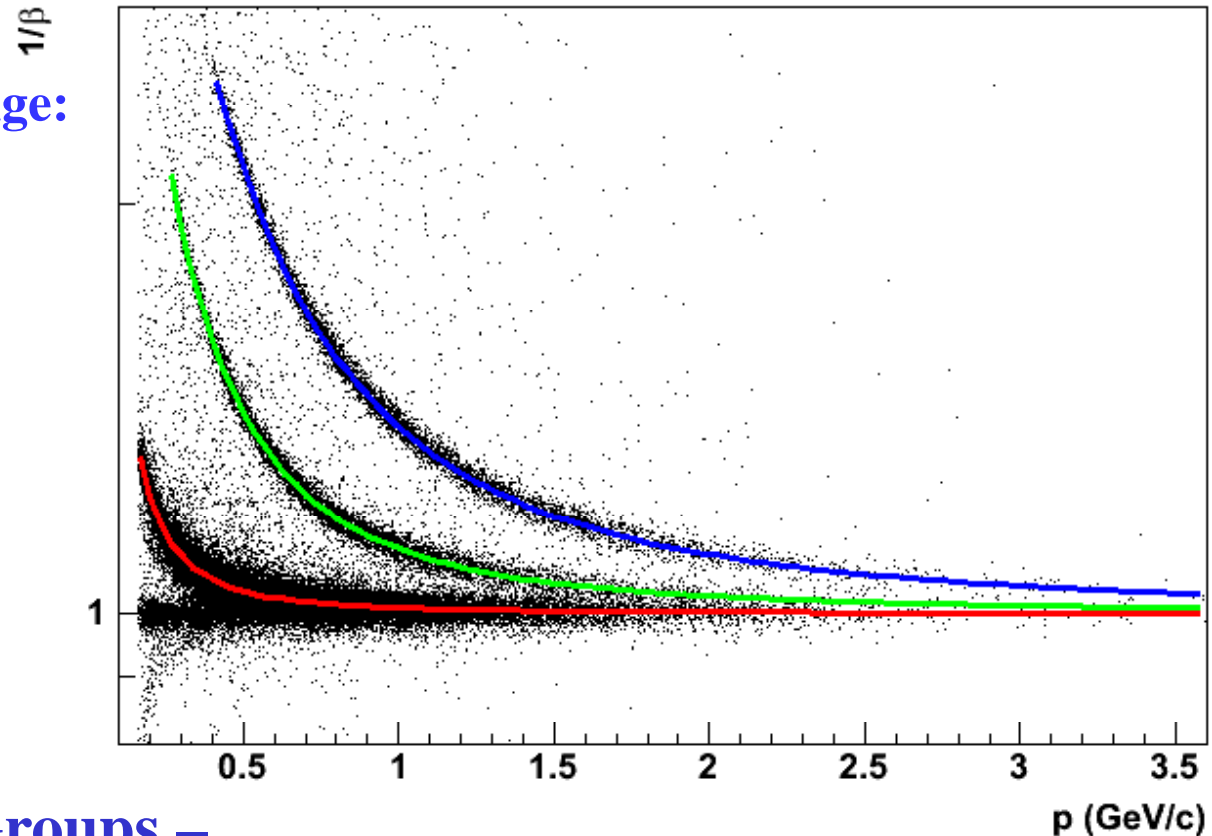
Chinese MRPC Works

TOFr PID (62GeV AuAu run)

TOF “alone” PID p_T range:

$\pi/K \sim 1.6 \text{ GeV}/c$,

$(\pi, K)/p \sim 3.0 \text{ GeV}/c$

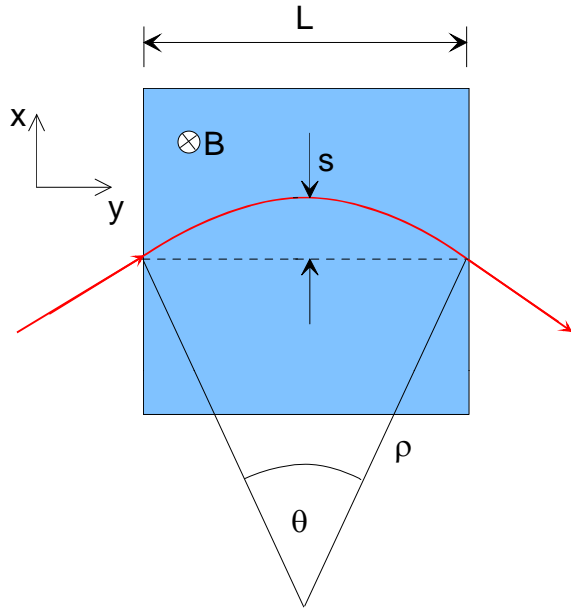


Chinese STAR Groups –

Shanghai Institute of Applied Physics, University of Science
And Technology of China, Tsinghua University, Hua Zhong
Normal University and Institute of Modern Physics at LanZhou

The End

Momentum Measurement in a Uniform Field



$$\frac{mv^2}{\rho} = q(v \times B) \rightarrow p_T = qB\rho$$

$$p_T \text{ (GeV/c)} = 0.3B\rho \text{ (T} \cdot \text{m)}$$

$$\frac{L}{2\rho} = \sin \theta/2 \approx \theta/2 \rightarrow \theta \approx \frac{0.3L \cdot B}{p_T}$$

$$s = \rho(1 - \cos \theta/2) \approx \rho \frac{\theta^2}{8} \approx \frac{0.3}{8} \frac{L^2 B}{p_T}$$

The sagitta $s = x_2 - \frac{1}{2}(x_1 + x_3)$ is determined by 3 measurements with error $\sigma(x)$:

$$\left. \frac{\sigma(p_T)}{p_T} \right|^{meas.} = \frac{\sigma(s)}{s} = \frac{\sqrt{\frac{3}{2}} \sigma(x)}{s} = \frac{\sigma(x) \cdot 8 p_T}{0.3 \cdot BL^2} \cdot \sqrt{\frac{3}{2}}$$

$$\left. \frac{\sigma(p_T)}{p_T} \right|^{meas.} = \frac{\sigma(x) \cdot p_T}{0.3 \cdot BL^2} \sqrt{720/(N+4)} \quad (N > 10)$$

TRANSITION AVALANCHE TO STREAMER

